Dissertation zur Erlangung des Doktorgrades

an der Fakultät für Chemie und Pharmazie

der Ludwig-Maximilians-Universität München

CDK5 interacts with STK3- A consequence to the Hippo Signaling

Mehak Passi

aus Chandigarh, Indien

2023

Erklärung

Diese Dissertation wurde im Sinne von §7 der Promotionsordnung vom 28. November 2011 von Frau Prof. Dr. Stefan Zahler betreut.

Eidesstattliche Versicherung

Diese Dissertation wurde eigenständig und ohne fremde Hilfe erarbeitet.

München, den: **05.04.2023**

Mehak Passi
_____

(Mehak Passi)

Dissertation eingereicht am: **22.02.2023**

1. Gutachter: Prof. Dr.Stefan Zahler

2. Gutachter: Prof. Dr. Angelika M. Vollmar

Mündliche Prüfung am: **15.03.2023**

If we knew what it was, we were doing, it would not be called research, would it? - Albert Einstein

Dedicated to lord Krishna and my family.

ੴ

Table of contents

ABSTRACT

1   Abstract

The Hippo-YAP/TAZ pathway is the most prevalent evolutionary conserved pathway from *Drosophila* to mammals and plays a key role in controlling organ size, cell growth, self-renewal, and tissue homeostasis. Hippo pathway consists of MST/LATS kinase module and YAP/TAZ-TEAD transcription module and is generally regulated by transcriptional activity of YAP and TAZ. YAP and TAZ are mechanosensory proteins that read a broad range of mechanical clues from shear stress of cell shape, contact, extracellular matrix rigidity and stiffness. In general, the Hippo pathway kinases are generally considered tumour suppressors while YAP/TAZ are considered Oncoproteins. Activation of transcription co-activators YAP/TAZ is inhibited by phosphorylation caused by LATS1/2 and MST1/2 kinases which results in cytoplasmic sequestration and degradation of YAP/TAZ. While unphosphorylated, YAP/TAZ translocate to the nucleus and bind to TEAD family transcription factors to induce gene expression. Hippo pathway is widely dysregulated in cancer and mechano-transduction of YAP and TAZ is critical for driving expression of genes involved in cancer progression and growth. Cyclin-dependent kinase 5 is an unusual member of the family of cyclin-dependent kinases, which is activated upon binding to non-cyclin p35 and p39 proteins. It is known to be widely involved in tumorigenic processes.

Through yeast two hybrid system we found a novel interaction between MST2 (STK3) and CDK5 which was further confirmed by co-immunoprecipitation experiments. In the current study, we aim to shed a light on the involvement of CDK5 in the Hippo pathway via interaction with MST2. We try to understand the relationship between CDK5 and Hippo kinases and how CDK5 influences the Hippo pathway cascade without being directly involved in it. We show how active YAP activity changes with CDK5 knockdown and overexpression. CDK5 also influences the expression of phosphorylated levels of upstream kinases of Hippo Pathway especially pLATS1 (thr1079). Expression of YAP target genes also get influenced where cells find a way to compensate for the reduced YAP activity by upregulating other mechanosensory pathways such as MRTF/.SRF. Our findings illustrate that it is not the kinase activity of CDK5 that is involved in the process.

However, it does act like a scaffold bringing the other proteins together and providing a platform for Hippo pathway cascade. Phosphoproteomics analysis brings the same picture out and shed light to the overall phospho changes with CDK5 knockdown and overexpression. Further phosphoproteomics results also reveal that CDK5 interact with DLG5 another upstream kinase and regulates the Hippo pathway via cross talk with several other signalling pathways especially MAPK signalling. Finally, CDK5 not only acts as a scaffold protein but also is involved assisting cross talk of Hippo pathway with other signalling cascades. Our findings might be useful for developing novel drugs which can target CDK5 and regulate Hippo signalling.

Keywords: - CDK5, Hippo pathway, YAP/TAZ, MST1/2, LATS1/2, kinases, overexpression, knockdown, MAPK.
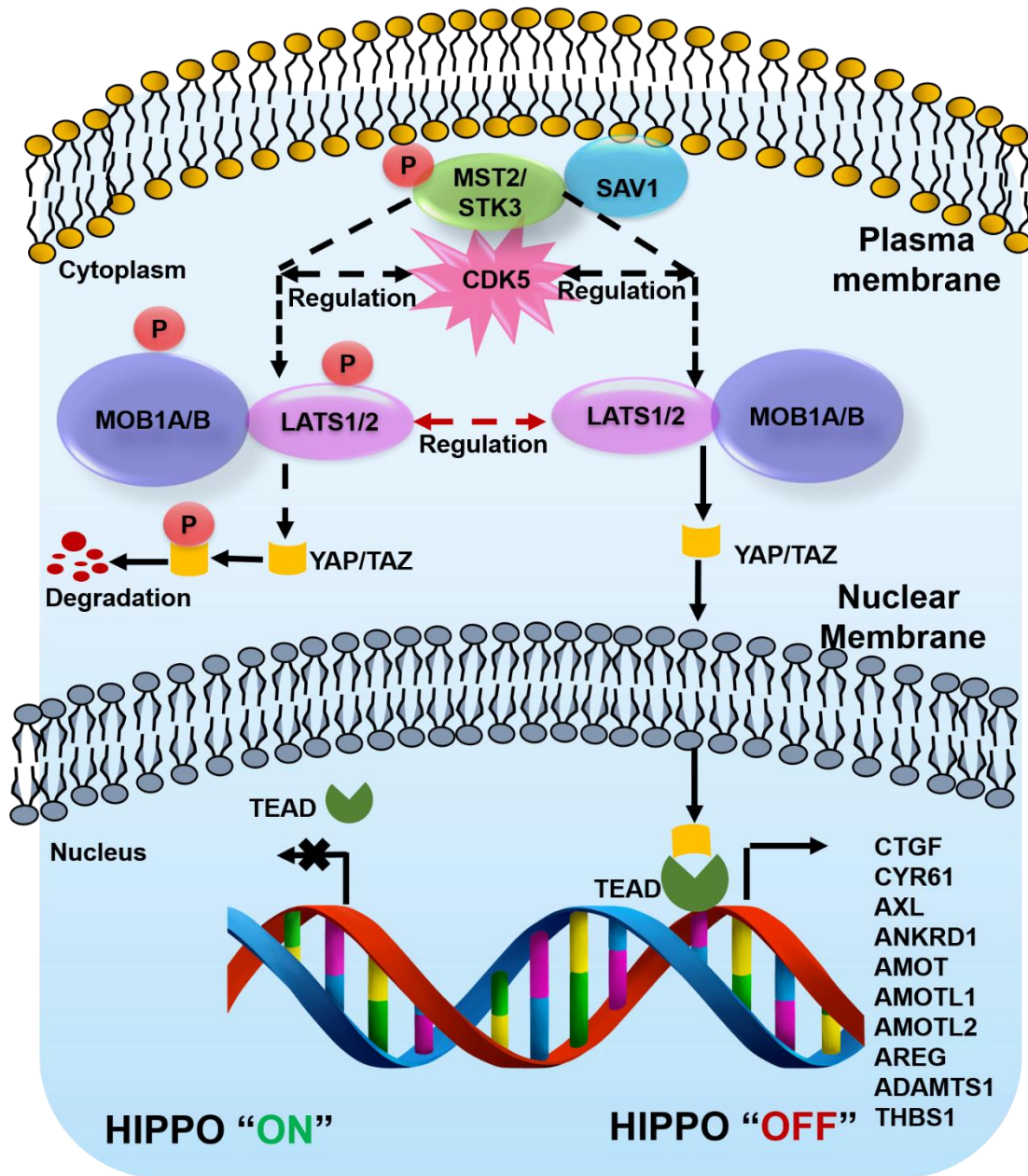
Figure 1 Graphical abstract representing the modulation of Hippo pathway by CDK5.

INTRODUCTION

2 Introduction

2.1 The Hippo signaling pathway – the overview

The Hippo signalling pathway is a well-conserved evolutionary pathway in higher-order vertebrates, which plays an important role in various processes, such as organ growth, cell proliferation, differentiation, and tissue homeostasis.[1, 2] It was first discovered in Drosophila melanogaster; however, its homologous components are found in mammals too. In this dissertation, we refer to the mammalian Hippo pathway. Many studies and The Cancer Atlas (TCGA) project in which from 9,125 tumour samples multi-omics profiling was performed indicated mutations, gene fusions, copy-number variations, mRNA expression and DNA methylation and an immense dysregulation of Hippo pathway genes in human cancers such as Hepatocellular carcinoma, skin cancer, osteosarcoma, ovarian carcinoma etc[3]. The Hippo pathway comprises core components and downstream effectors, where core kinases act as a tumour suppressor whereas downstream effectors YAP/TAZ act as oncogenic proteins. The core components of the Hippo pathway are serine/threonine kinases, sterile 20-like kinases, 1/2 (MST1/2), and large tumour suppressor 1/2 (LATS1/2). MST Kinases undergo auto-phosphorylation at the auto-activation loop of MST dimer, MST1 at Thr183 and MST2 at Thr180. The SARAH domain is referred to as the distinctive close-coiled structure of the carboxy terminus of MST kinases (named after three genes that contain the homologous structures – Salvador 1/WW45), RASSF1-6 and Hippo (MST1/MST2)[2]. Homo-/ heterodimerization of MST1/MST2 is mediated by the SARAH domain where MST1/MST2 heterodimer forms a complex with Salvador 1 (SAV1), a SARAH domain-containing protein. A complex between LATS1 and LATS2 kinase and MOB kinase activators 1A and 1B is formed too [4]. MST1/MST2 kinases phosphorylate LATS1 and LATS2 at Thr 35 and Thr12, and MOB1A and MOB1B at Thr35 and Thr12. These phosphorylation events lead to an interaction of MOB1A/MOB1B to LATS1/LATS2 which further leads to autophosphorylation of LATS1/LATS2 at the activation loop (Ser909 at LATS1 and Ser872 at LATS2). Overall, these double phosphorylation events lead to LATS1/LATS2 kinase activation. Hippo pathway downstream effectors YAP and TAZ are the key

substrates of LATS kinases [3]. YAP is the first protein identified within the WW domain that is the key transcriptional regulator and TAZ is a YAP paralog with about 44% identity to YAP. There are about 5 YAP (Ser61, Ser109, Ser127, Ser164 and Ser381) and 4 TAZ (Ser66, Ser89, Ser117, and Ser311) HXRXXS-T motifs, which are phosphorylated by LATS1/LATS2[5]. This phosphorylation of YAP and TAZ by LATS kinases leads to cytoplasmic sequestration of YAP/TAZ or ubiquitin-mediated protein degradation[6]. YAP/TAZ translocate to the nucleus if not phosphorylated by LATS/LATS2 where they bind to the TEAD transcription factor family (TEAD1-4) to mediate gene expression that is involved in cell growth, proliferation, migration, and survival, such as CTGF connective tissue growth factor and CYR 61 cysteine-rich angiogenic inducer 61 [3]. YAP/TAZ also interact and bind to other transcription factors such as RUNT-related transcription factor (RUNX1 and RUNX2), T-box transcription factor 5 (TBX5), SMAD1, SMAD2/3 and P73 [7]. YAP has also been shown to interact with the intracellular domain (ICD) of

ErbB4, which is one of the members of the epidermal growth factor receptors in the nucleus to modulate the expression of genes involved in proliferation, differentiation, and development [8]. Loss of any core components of the Hippo pathway such as Merlin, MST1/MST2, Salvador-1, LATS1/2, and MOB1A/MOB1B lead to upregulation of YAP/TAZ-TEAD level subsequently increasing the levels of target gene expression involved in cell proliferation and tissue growth[3] [9].
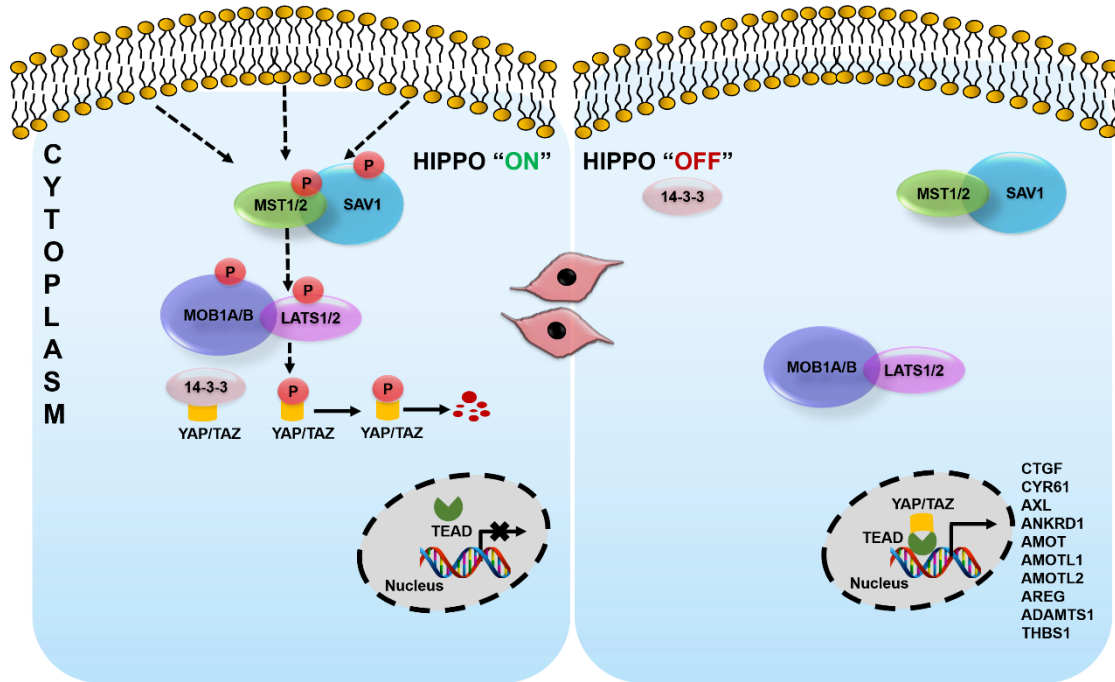
Figure 2 Hippo signalling cascade and its major effectors, upstream kinases STK3 (MST1/2), LATS1/2 and Oncoproteins YAP/TAZ with left panel demonstrating when Hippo signalling is on how phosphorylation events lead to sequestration of YAP/TAZ in cytoplasm and its inactivation. Right panel demonstrates in event of inhibition of Hippo signalling, how YAP/TAZ enter the nucleus and leads to transcription of genes responsible for uncontrolled cell proliferation and growth.

2.2   MST Kinases

Mammalian sterile twenty (MST) kinases are MST1 (STK4) and MST2 (STK3) of the GCK germinal centre kinase (GCK)II subfamily, and MST3 (STK24), MST4 (STK26), and SOK1/YSK1 (STK25) of the GCK III subfamily. In the thesis, we talk about MST2 i.e, STK3 in general [10]. The human MST2 comprises 491 amino acids and is identical to MST1 about 75%. It consists of the SARAH domain at C-terminus, which is a unique coiled-coil structure allowing the binding with other proteins sharing the same domain. The SARAH domains comprise of 50 amino acids and its catalytic domain is linked together by a segment of the caspase 3 cleavage motif. These SARAH domains also help in the homo and heterodimerisation of MST2.

2.2.1 Regulation

The activity of MST2 can be regulated in various modes. For instance, its catalytic activity can be abolished by mutations in two critical residues, one with an ATP binding site at Lys56 and 2nd a catalytic site at Asp156. Any kind of mutations in the SARAH domain also led to a subsequent decrease in kinase activity, as it is crucial for phosphorylation. Autophosphorylation of MST2 by other kinases such as MAP4K and TAOK leads to a stronger kinase activity of MST2 by forming a homodimer. On the other hand, heterodimerization of MST1/MST2 by Ras-GTP hampers its activity and hence the activation of the Hippo pathway[11].

Other proteins, such as the RAS-associated domain-containing proteins 1-6 (RASSF1-6) with SARAH domains bind to MST2 and form a hetero dimer and activate MST2 [12]. Overexpression of RASSF1 has been associated with overexpression of MST1/MST2. The interaction between MST2 and Sav1 is also very prominent, but it is yet unknown whether it promotes autophosphorylation or recruitment of other kinases such as TAO1[13]. In addition, there have been studies in hepatocytes demonstrating that caspase 3 cleavage in hepatocytes regulates MST2 by removing the SARAH domains. This gives MST2 unrestricted access to the nucleus where it promotes the progression of apoptosis, maintaining the replicative quiescence and/or of the differentiated state in hepatocytes. Akt also regulates the activity of MST2 by inhibiting its phosphorylation at residue Thr117 in response to insulin-like growth factor -1 (IGF1) [4]. This demonstrates a cross-regulation between the Hippo pathway and insulin-IGF signalling. MST2 negatively regulates by binding to it and not via its kinase activity.

Raf1 also inhibits the activity of MST2 by binding to the SARAH domain hindering its homo and heterodimerisation and activation in a kinase-independent manner. The binding of Raf1 and MST2 is promoted by the phosphorylation of Raf1 (Ser259) by Akt or LATS1[14]. The interaction of MST2-Raf1 is disrupted by the phosphorylation of MST2(Tyr81) by subsequent activation of MST2 by its homodimerization. MST2 is also known to be activated during the G2/M phase of mitosis, however, the mechanism underlying this is unknown yet [4, 15].
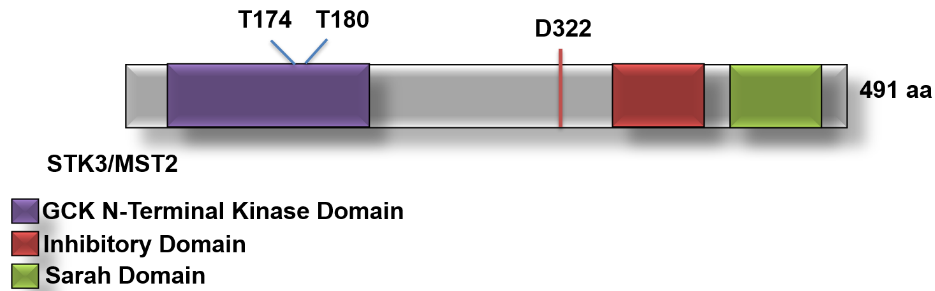
Figure 3 Domain structure of STK (MST2), with different colours representing different domains as mentioned.

2.3   YAP/TAZ

YAP is characterised by one or two WW domains containing two tryptophans, a coiled-coil domain, a PDZ interaction motif and an SH3 interaction motif **(Figure 3)**. YAP/TAZ does not contain any DNA binding domain [16]. Therefore, they need to bind to transcription factors to associate with different promoters of the target genes. TEAD/TED are the most prominent family of transcription factors (TFs) which are present in almost every tissue, even in differentiated ones, and they act as the most common family of transcription factors interacting with YAP/TAZ [17]. YAP/TAZ generally act by interacting with SWI/SNF chromatin-remodelling complex and by subsequent recruitment of methyl transferase complex nearby these TEAD/TED transcription factors. The binding of WW domains of YAP/TAZ with the PPxY motif of the components of both complexes, chromatin-remodelling and methyl transferase complex mediates the interaction. The interaction of YAP/TAZ with these complexes increases histone methylation and subsequent transcription of genes. YAP/TAZ association with TEAD TFs can also function as a transcriptional compressor of target genes [18].
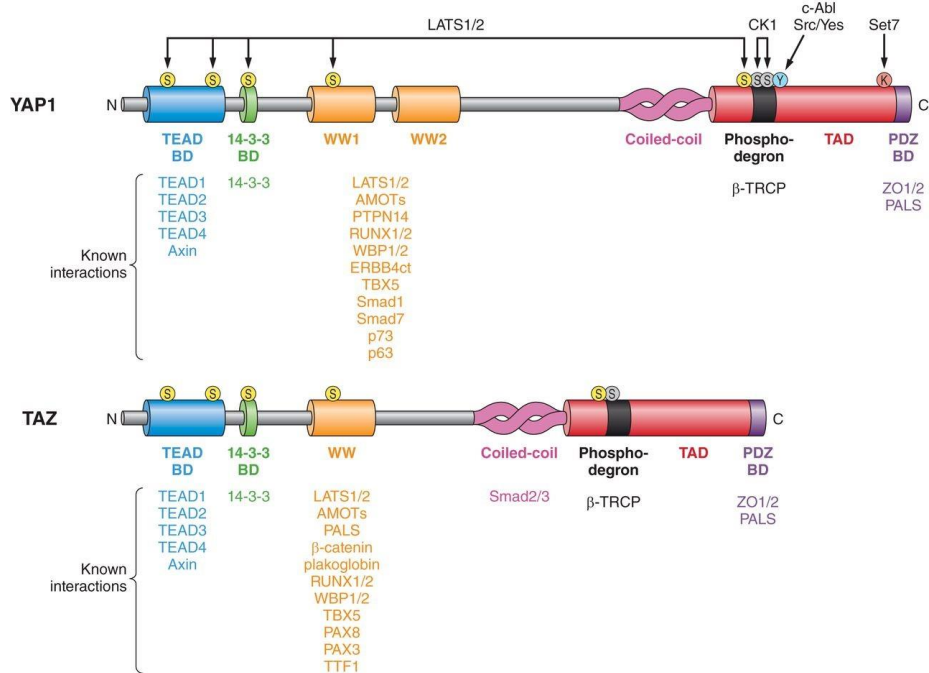
Figure 4 Schematic representation of YAP domains with relevant phosphorylation sites and the known interacting partners. The figure was *adapted from* Piccolo, Stefano, Sirio Dupont, and Michelangelo Cordenonsi. "The biology of YAP/TAZ: Hippo signaling and beyond." *Physiological reviews* (2014).

2.4   YAP/TAZ regulation by the Hippo pathway

Apical basal polarity separates the adherens junctions and tight junctions and is connected to various signalling pathways and controls cell development and tissue growth (Figure 2).Many recent studies have found that many proteins associated with cell polarity and adhesion control and regulate the activity of YAP/TAZ in the Hippo pathway [19]. In mammals, a tight junction (TJ)- associated scaffold protein called angiomotin has emerged as a critical regulator for the hippo pathway. Amot comprises PY- and PDZ- binding domains and interacts with YAP/TAZ through PPXY motif and WW domain interactions promoting its cytoplasmic retention [20]. Additionally, Amot interacts with both LATS1/2 and MST1/2 and suppresses the activity of YAP/TAZ in turn. Another polarity protein localized to epithelial junctions, Scribble has been shown to interact with and inhibit TAZ [5]. Zonula occludens-2 (ZO-2), a tight junction cytoplasmic scaffold protein interacts with the C-terminal PDZ domain of YAP/TAZ and promotes its nuclear translocation. α-Catenin, a major component of adherens junctions (AJs) functions as a tumour suppressor by negatively regulating YAP activity during epidermal stem cell proliferation and

tissue expansion [21]. It had been demonstrated that deletion of α-Catenin in the hair follicle stem cells progresses to skin cancer because of the constitutive nuclear localisation of YAP. E-cadherin/catenin–dependent contact inhibition of proliferation via YAP inhibition also requires the Hippo pathway as it acts as a switch. Another AJ component, protein tyrosine phosphatase 14 (PTPN14) also contributes to the cytoplasmic retention of YAP by directly interacting with it [22]. Therefore, the apical cell polarity complex, cadherin/catenin and adherens junctions proteins are important regulators of Hippo signalling to suppress cell proliferation and tumorigenesis[23].

2.5   Regulation of the Hippo pathway by extra cellular ligands and cellular stress

The Rho family of proteins importantly Rho GTPases including RhoA, Rac1 and Cdc42 play an important role in Hippo pathway regulation and link extracellular stimuli such as membrane receptor signalling and mechano transduction to YAP /TAZ activity [24]. The Hippo pathway is regulated via Rho GTPases by various G protein-coupled receptors (GPCRs) and their associated heterotrimeric G protein. LATS1/2 is inhibited by Serum-borne lysophosphatidic acid (LPA) and sphingosine 1-phosphate (S1P), which act as ligands for the Gα12/13–coupled receptor, and its downstream RhoA signalling [25]. Thrombin and Thromboxane A2 and Kaposi sarcoma-associated herpesvirus also activate YAP via Rho GTPases. YAP/TAZ is also activated by Serum-borne lysophosphatidic acid (LPA) and sphingosine 1-phosphate (S1P) act as ligands for the Gα12/13–coupled receptor, and its downstream RhoA signalling. Similarly, YAP/TAZ is also activated by Gαq/11-coupled GPCR ligands, such as endothelin-1 and estrogen [26]

In contrast, activation of PKA by cAMP upon stimulation with Gαs-coupled receptors inhibits Rho GTPases, which in turn activates LATS kinase activity [27]. Additionally, RhoGTPases link ligand stimuli to the Hippo pathway through F-actin formation. Modulation of actin polymerization by Rho GTPases and actin capping proteins affect the YAP activity in mammalian cells [28].

β-catenin is the key transcriptional co-activator in Canonical Wnt signalling. YAP/TAZ interact with β-catenin and inhibit Wnt signalling by sequestering it in the

cytoplasm. YAP/TAZ are essential for the formation of the β-catenin destruction complex. YAP also modulates the TSC-mTORC1 pathway by promoting mTORC1 activation via TEAD-induced LAT1 amino acid transporter[18, 29].

Hippo pathway activation by cellular stresses is considered an important tumour suppression mechanism. There are some studies which demonstrate that YAP/TAZ activity is affected in response to cellular stress caused by various factors such as osmotic pressure, and UV radiation[30]. For instance, MAPK including JNK and p38 also modulate the hippo pathway under stress conditions. JNK and p38 MAPK also upon activation by UV radiation, phosphorylate and potentiate YAP[31]. TEAD cytoplasmic translocation is also promoted by p38 which suppresses the YAP-driven cancer cell growth. Nuclear accumulation of YAP is also promoted by its phosphorylation at Ser128 by NLK and its disruption with the 14-3-3 protein family during osmotic stress[32].

2.6   Interaction of the Hippo pathway with other pathways

The Hippo pathway crosstalks with many pathways such as the WNT–β-catenin pathway, BMP, transforming growth factor-β (TGFβ), G-protein-coupled receptor GPCR, notch and phosphoinositide 3-kinase (PI3K)–RACα serine/ threonine-protein kinase (AKT) signalling pathways.

By cross talking with other pathways, it regulates the expression of genes which act as of many epigenetic factors, mechanical and hormonal signals, cell-cell contact, cell polarity and cytoskeleton which play an important role in cell proliferation, survival, differentiation, migration, and metabolism[33]. For instance, YAP is regulated by multiple G protein-coupled receptors through their influence on Rho activity. Wnt signalling interacts with Hippo signalling by several points such as interactions of YAP with dishevelled and Adenomatous polyposis coli and the coregulation of downstream genes by YAP and β-catenin. Hippo and BMP pathways crosstalk via interactions between YAP and SMADs[25]. YAP activity is also influenced by EGFR and related pathways through multiple mechanisms. YAP activity is also influenced JNK signalling. YAP and Hedgehog signalling also interact in multiple tissues, including the intestine, skin, and nervous system.
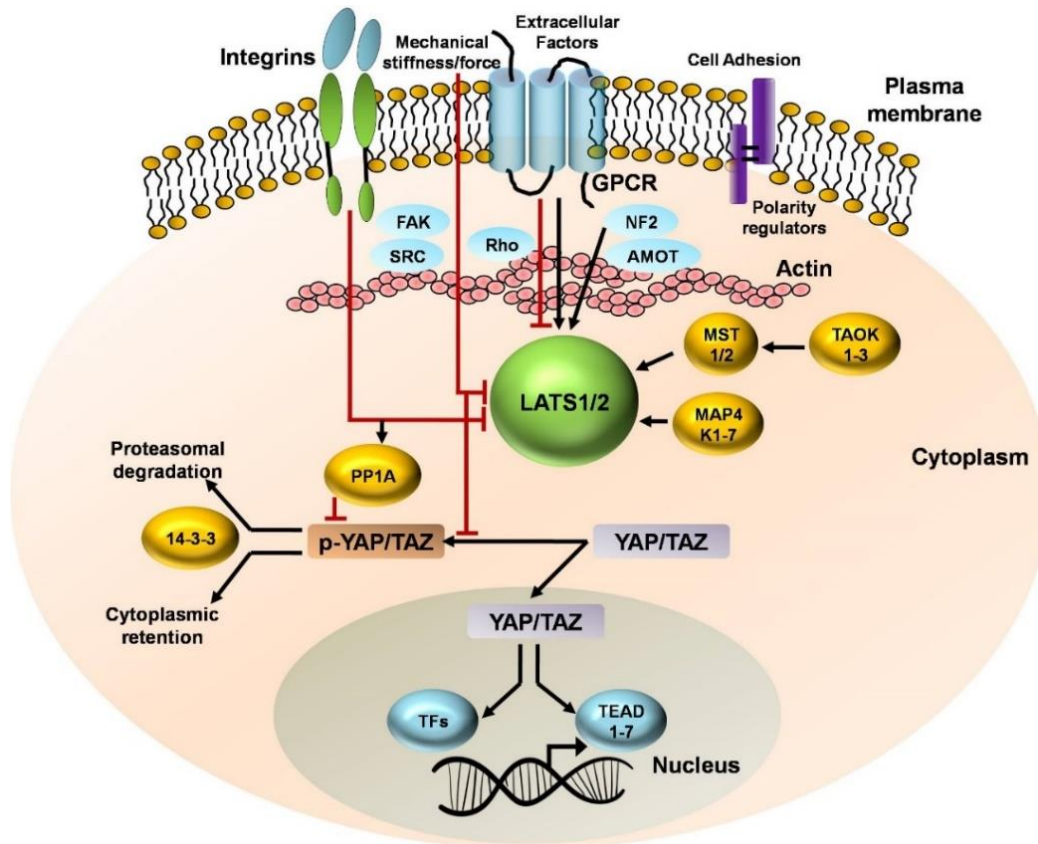
Figure 5 Various external and mechanical factors regulating the activity of YAP/TAZ.
LATS1/2 phosphorylate YAP/TAZ and regulate its activity. Phosphorylated YAP/TAZ associate
with 14-3-3 proteins and are retained in cytoplasm and are subjected to proteasomal degradation.
Several external factors such as MST, MAP4K and TAOK families of kinases phosphorylate and
activate LATS1/2. Several external factors such as cell polarity, cell adhesion regulators facilitate
altered actin dynamics and Hippo pathway factor association to promote LATS1/2 mediation
YAP/TAZ regulation. G protein coupled receptors (GPCRs), mechanical cues and signals
transduced by the extracellular matrix and matrix-binding integrins can inactivate LATS1/2 to
induce dephosphorylation of YAP/TAZ via PP1A activation, leading to hypo phosphorylated
YAP/TAZ which accumulates in the nucleus and bind to TEAD family to carry out gene expression.
This figure was modified from, Dey, Anwesha, Xaralabos Varelas, and Kun-Liang Guan. "Targeting
the Hippo pathway in cancer, fibrosis, wound healing and regenerative medicine." *Nature reviews
Drug discovery* 19.7 (2020): 480-494**.**

2.7 The Hippo pathway in cancer biology

Aberrations of the Hippo pathway are associated with the hallmarks of
oncogenesis such as hyperproliferation, cellular invasion, and metastasis and the
role in cancer maintenance and chemotherapeutic resistance mechanisms.
Analysis of over 9000 tumours has revealed that YAP and TAZ are frequently
amplified in the head, neck, and gynecologic cancers while the upstream
regulators LATS1/2 and NF2 are commonly mutated in gastrointestinal and

gynaecologic cancer and mesotheliomas [1, 34]. All of these are highly associated with overexpression of nuclear YAP and TAZ and elevated TEAD expression, but the mechanism of overexpression remains unknown. The crosstalk with chromatin regulators and other signalling pathways is also responsible for the dysregulation of the Hippo pathway[7].

2.8 Biological basis of the Hippo pathway in tumorigenesis

2.8.1 Cell proliferation and cell cycle

One of the most important hallmarks of cancer is uncontrolled cell proliferation. Cells in adult tissues control their cell cycle progression to maintain homeostasis of cell number and organ size. YAP and TAZ control the expression of genes involved in cell cycle regulation and promote cell proliferation. For instance, YAP activation upregulates the transcription of cell cycle-positive regulators such as CCND1 and FOXM1 promoting malignant mesothelioma cell proliferation. Moreover, YAP/TAZ also maintain their activation by the self-sustaining positive loop[35, 36].

2.8.2 Apoptosis

Programmed cell death plays a key role during the development of a tissue and its imbalance is another cancer hallmark. It has been reported that overall active YAP confers resistance to apoptosis induced by cancer chemotherapy such as RAF and MEK inhibitor therapy[37] . In the case of BRAF- or RAS-mutant cancers inhibition of YAP and oncogenic MAPK signalling leads to better therapeutic effects by synergistic induction of apoptosis[38].

2.8.3 Cell-cell contact

Contact inhibition is important to maintain appropriate organ size and tissue homeostasis. Cell-Cell contact inhibits the core kinase activity of the hippo components and YAP/TAZ nuclear localisation. Stiffening of the extracellular matrix or mechanical stretching of E-cadherin cell-cell junctions lead to activation of YAP/TAZ [35].Hyperactive YAP and dysregulation of the Hippo pathway can result

in continuous proliferation and uncontrolled growth by overcoming contact inhibition[1]

2.8.4 Invasion and metastasis

The ability to do local invasion and distant metastasis enables the cancer cells to migrate into other tissues. Dysregulation of the Hippo pathway contributes to metastasis in various cancers. YAP/TAZ activation induces an EMT phenotype by coordinating with EMT-orchestrating proteins such as ZEB1 [39]. It is accompanied by the downregulation of epithelial markers such as E-cadherin and occludin and the upregulation of mesenchymal markers vimentin and N-cadherin. YAP also promotes the expression of leukocyte-specific integrin β2 (ITGB2) and enhances cell invasion through the endothelium which is a key barrier to metastasis[40]. F-actin/G-actin turnover is very important for cell migration and cytoskeletal rearrangement. It has been demonstrated that YAP activates ARHGAP29 expression, which inhibits the RhoA-LINK -cofilin pathway resulting in the destabilization of F-actin to promote metastasis[41].

2.8.5 Inflammation

Inflammation is an important mechanism for tissue repair but is also a hallmark of tumorigenesis. In the intestine, YAP is activated by IL-6-gp130 signalling. LATS-dependent YAP activation is found in both, repair of damaged tissues and cancer. There the link between chronic inflammation and YAP tumorigenesis is not excluded [23, 42].

2.8.6 Immune response

Immune surveillance prevents cancer initiation by the destruction of nascent tumours. Overexpression of YAP/TAZ endorses the tumoral cells escape from immune surveillance in epithelial cells [43]. For instance, M2 polarization of macrophages is associated with tumour development, invasion, and metastasis. The studies in mouse models of liver cancer have demonstrated that the activation of YAP in a single hepatocyte is efficient to promote the recruitment and activation

of macrophages[44]. This occurs due to the expression of YAP-mediated target gene C-C motif chemokine ligand 2 (Ccl2) [45].

Furthermore, in prostate and pancreatic cancer, YAP/TAZ is crucial for the recruitment of myeloid-derived suppressor cells (MDSCs). MDSCs inhibit cytotoxic T-cells and favour the formation of a supportive tumour microenvironment and angiogenesis[46, 47].

Also, YAP stimulates the production of cytokines such as IL-6, macrophage colony-stimulating factors (CSF1), granulocyte-macrophage colony-stimulating factor (CSF2), granulocyte colony-stimulating factor CSF3 and C-X-C motif chemokine ligand 5 [48].

Surface expression of the programmed cell death ligand 1 (PDL1) is a known mechanism used by tumour cells to escape T-cells surveillance. YAP/TAZ could transcriptionally control its expression in some cancer cells such as melanoma, lung, and mesothelioma cells[49].

2.8.7 YAP/TAZ Mechanobiology

The subcellular distribution of YAP and TAZ accounts for their regulation with their activation entailed in their YAP and TAZ nuclear distribution. The cellular distribution of YAP and TAZ is controlled by a variety of factors such as cell shape, rigidity, and topology of the ECM substrate and by shear stress[50].

For instance, in the case of cells experiencing low levels of mechanical forces most of the YAP and TAZ are in the cytoplasm especially in rounded cells attached to a soft ECM (typically <1.5 kPa) or to a small adhesive area[1]. In the cells perceiving higher levels of mechanical forces, such as cells cultured on rigid substrates (typically at > 5-10 kPa) most of YAP and TAZ seem to be in the nucleus. On the rigid substrate, cells experience high levels of deformation and cytoskeletal tension[18].

Moreover, various regimen of cell stretching, such as deformations, rigidity and deformability of ECM supporting cellular outgrowths in 3D for example organoids also mechanically regulate YAP and TAZ[51].

YAP and TAZ signalling is not only about reading cell mechanics but is also very crucial for mediating biological effects associated with mechanical signalling in each biological system, such as proliferation, differentiation, and wound healing. The integrity of the actin cytoskeleton is required for YAP and TAZ mechanotransduction, and it can be abolished by F-actin inhibitors. It relies on the specific organisation of the F-actin cytoskeleton. It is revealed by the potent inhibitory effects of F-actin capping proteins such as capping actin protein of muscle Z-line (CAPZ) and actin depolymerizing factor (ADF)/cofilin as well as F-actin regulatory proteins such as angiomotin, spectrins and tight junction protein zonula occludent proteins 2 (ZO2) [50].

In addition, YAP and TAZ activation have also been linked to actin contractility and increased tension of the actin cytoskeleton. However, the exact mechanisms of how YAP and TAZ mechanotransduction is affected by the actin cytoskeleton is still unknown [52]. Mechanosensory protein networks such as integrins and adherens junctions, adaptor proteins such as vinculin and talins, focal adhesion kinase and the Src family kinases, which are responsible for propagation and preservation of information within the cytoskeleton also regulate YAP and TAZ[53]. Finally, through actomyosin contractile network and cytoskeletal remodelling cells dynamically respond to external forces with proportional cell-generated force. In some cell types inhibitors of myosin light chain kinase and RHO-associated protein kinase (ROCK), inhibits the activation of YAP by stiff ECM [54]. The cytoskeleton is restructured by activation of RHO GTPases by integrin activation. RHO signalling is essential for YAP and TAZ activity and has been exploited in various systems either genetically or by using RHO inhibitors [55].
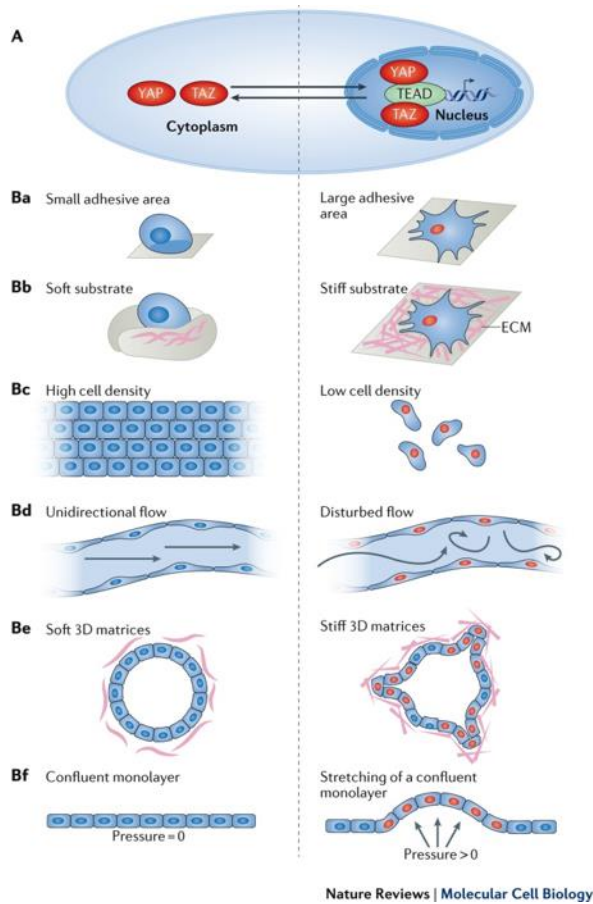
Figure 6 Factors regulating YAP/TAZ activity: left panel describing the factors which lead to lower activity of YAP/TAZ and right panel describing factors leading to higher YAP/TAZ activity. Active YAP/TAZ is demonstrated by red colour. The figure is adapted from Panciera, Tito, et al. "Mechanobiology of YAP and TAZ in physiology and disease." *Nature reviews Molecular cell biology* 18.12 (2017): 758-770.

2.9 CDK5

Cyclin-dependent kinase 5 is an atypical cyclin-dependent kinase, which is mainly characterised by its role in the central nervous system rather than in the cell cycle. CDK5 has emerged as one of the crucial regulators of neuronal migration in the development of the central nervous system[56]. CDK5 is expressed in mammals and cultured cells. Like other CDKs, CDK5 alone exhibits no enzymatic activity and requires association with a regulatory partner for activation. It is co-localised with its substrates and activators and is activated by the binding of subunits[57].

CDK5 is mainly activated by binding to the non-cyclic activators p35 or p39, and phosphorylates substrates on serine or threonine residues within the consensus

motif S/TPXH/K/R[58]. CDK5/p35 and CDK5/p39 are active forms of kinase but exhibit relatively low catalytic activity. Phosphorylation of Ser159 on the T loop of CDK5 and the binding of p35 is necessary to exhibit the maximum activity of CDK5[59]. CDK5 is also activated by binding to cyclin 1 and the CDK5/cyclin 1 complex is associated with resistance to cisplatin treatment. Cleavage of CDK5 cofactors by calpain produces p25 or p29 by removing 100 amino acids from CDK55/p35 complexes containing a cdk5 binding domain. The resulting CDK5/p25 or CDK5/p29 holoenzymes are more soluble and can access cytoplasmic and nuclear substrates. CDK/p25 and CDK5/p35 have been linked to tumorigenesis, and CDK5/p25 seems to be a more toxic form of CDK5 linked to neurodegenerative diseases[60].
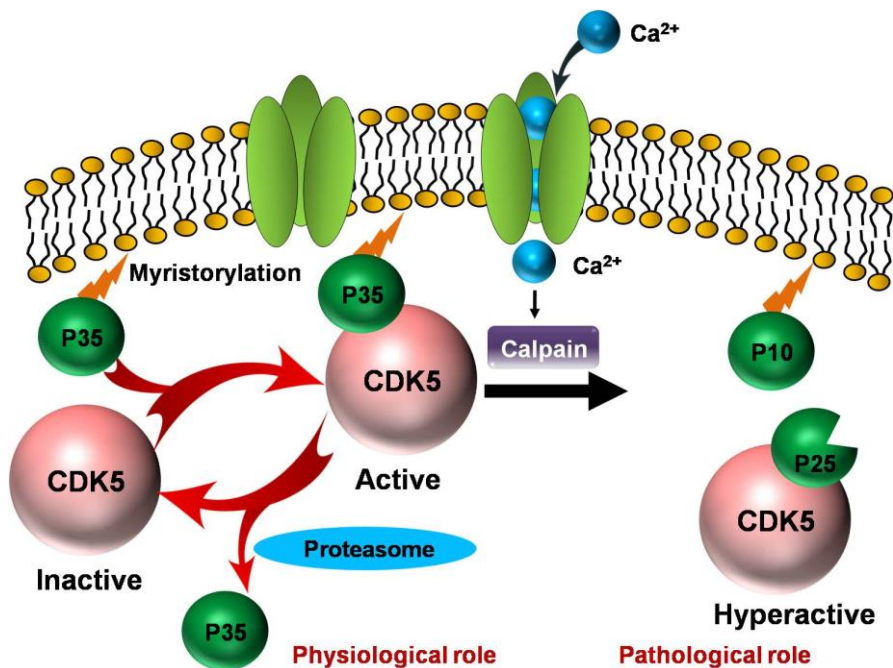
Figure 7 CDK5 lifecycle. Upon binding with p35, CDK5 undergoes autophosphorylation with the subsequent ubiquitylation and degradation or alternatively calpain can cleave p35 in response to elevated cytosolic Ca^{2+} to form p25. This figure was modified from, "Do, Phuong Anh, and Chang Hoon Lee. "The role of CDK5 in tumours and tumour microenvironments." *Cancers* 13.1 (2020): 101.

2.9.1 CDK5 and Cancer

There is a lot of evidence suggesting the important role of CDK5 in human cancers. Many genetic variations of genes associated with p35/p39 and CDK5 such as single-nucleotide polymorphisms or gene amplification can be found in many cancers [56]. mRNA expression and protein levels of CDK5 and its activators are dysregulated in many cancers.

There are many cases of CDK5 involvement in cancer and tumorigenesis. In head and neck squamous cell carcinoma, aberrant overexpression of CDK5 significantly induces tumour cell motility and epithelial-mesenchymal transition. Hyperactivation of CDK5 induces proliferation and clonogenic growth of HCC[61].

In Medullary Thyroid cancer (MTC) transcription factor E2F is released when retinoblastoma protein is phosphorylated by CDK5 and promotes the transcription of genes needed in cell cycle progression.[62]

Similarly, in MTC and prostate cancer CDK5 is involved in the phosphorylation of STAT3, which in turn enhances the transcription of target genes involved in cancer growth. In HCC, overexpression and hyperactivation of CDK5 play an oncogenic activity by inducing proliferation and clonogenic growth of HCC[63]. Androgen receptor is another substrate of CDK5, which is phosphorylated and stabilized by CDK5. CDK5 mediate prostate cancer progression through STAT3 and AR signalling [64].

In breast cancer cells, both p35 and CDK5 are upregulated and hyperactivated after treatment with transforming growth factor beta 1 (TGF-β1) leading to subsequent EMT and cancer cell motility by phosphorylating FAK, which is known to be involved in cellular adhesion [65]. In pancreatic cancer cells, CDK5 plays an important role and Ras-RAL signalling by downregulating active forms of Ral and Rho proteins, both of which play an important tumour progression and metastasis. CDK5 also supports metastasis formation by regulating the actin cytoskeleton, focal adhesions, and the formation of invadopodium [66].

Finally, CDK5 has also been known to be a contributor to angiogenesis. Angiogenesis is the process by which new blood vessels form from the pre-existing ones to ensure the delivery of nutrients and oxygen to growing tumours subsequently allowing the removal of metabolic waste and together with lymphatic vessels, providing an escape route for cancer cell migration to the metastatic site.

CDK5 is a master regulator of angiogenesis in the least some cancers. It acts as a crucial regulator of endothelial cell survival. For instance, CDK5 overexpression triggers cell proliferation and angiogenesis where CDK5 inhibition with roscovitine arrests it and causes apoptosis. CDK5 regulates lamellipodia formation and contributes to endothelial cell migration by remodelling the actin cytoskeleton via regulation of the monomeric GTPase Rac1. CDK5 even regulates the expression of angiogenic molecules such as hypoxia-inducible factor 1/ (HIF1/) target gene, vascular endothelial growth factor (VEGF)-A and VEGF-receptor which are essential for the formation of new blood vessels. Angiogenic factors such as fibroblast growth factor secreted by tumour cells regulate the CDK5 expression in endothelial cells[62]

With the apparent role of CDK5 in endothelial cell physiology and tumour angiogenesis, it is a target for antiangiogenic treatment with new anti-CDK5 drugs being discovered. Other potential downstream targets of CDK5 have been identified, such as HIF1/ and Notch. With the recent advances, the role of CDK5 in supporting tumour development and spread is becoming clear. Apart from being dysregulated during tumorigenesis in various cancers, CDK5 is also associated with cell cycle suppressor and anti-tumoral activities[67] .

CDK5 is involved in the initiation of DNA damage response and DNA damage repair. Many DNA agents have been shown to induce p25 upregulation and CDK5 upregulation to repair DNA[67]. For instance, CDK5 is involved in the phosphorylation of checkpoint-activating kinase Ataxia-telangiectasia mutated (ATM) and the replication protein A (RPA)-32, two proteins involved in the DDR and DNA repair. Thus, the co-administration of CDK5 inhibitors has also been suggested for a better outcome of DNA damage-based therapy[68].

2.9.2   CDK5 and Hippo pathway

There have been many studies demonstrating the alterations of ECM in tumoral tissues. A major component of ECM is collagen, which has been reported to be altered or denatured. In this context, there is a study about the HU177 epitope, a cryptic regulatory region of collagen, which is exposed upon denaturation[69]. In melanoma targeting, this epitope has been shown to reduce angiogenesis and cell migration. Interestingly blocking of the interaction of cells with HU177 diminishes the phosphorylated levels of CDK5 indicating that CDK5 is involved in this process. Furthermore, inhibition or knocking down of CDK5 lead to the reduction of nuclear YAP levels suggesting the involvement of YAP too. This whole study indicated that the HU177 epitope might regulate the angiogenesis and cell migration of melanoma cells by controlling YAP nuclear levels in a CDK5-dependent manner[69]. However, more studies are required to elucidate this connection. Furthermore, there is another study, which demonstrated that CDK5 activates Hippo signalling via TAZ and participates in tumorigenesis and radio resistance in lung cancer. Depletion of CDK5 leads to the downregulation of TAZ and attenuates Hippo signalling impairing lung cancer progression and radio resistance. Therefore, there seems to be a sort of connection between CDK5 and the Hippo pathway.

In the current dissertation we aim to demonstrate a link between CDK5 and Hippo pathway. We demonstrate how. CDK5 Interacts with STK3 and varies the consequences of Hippo signalling.

MATERIALS AND METHODS

3 Materials and Methods

3.1 Materials

3.1.1 Reagents

Reagent	Producer
Calcein-AM	Biomol GmbH, Hamburg, Germany
Collagen G	Biochrom AG, Berlin, Germany
Complete®	Roche Diagnostics, Penzberg, Germany
Dimethylsulfoxide (DMSO)	Sigma-Aldrich, Taufkirchen, Germany
Dithiothreitol (DTT)	Sigma-Aldrich, Taufkirchen, Germany
Dulbecco's Modified Eagle Medium (DMEM)	PAA Laboratories, Pasching, Austria
Ethylenediaminetetraacetic acid (EDTA)	Sigma Aldrich, Taufkirchen, Germany
Fetal calf serum (FCS)	Biochrom AG, Berlin, Germany
Glycerol	Applichem¸ Darmstadt, Germany
High-Capacity cDNA Reverse Transcription Kit	Applied Biosystems, Waltham, USA
Live Cell Imaging Solution	Life Technologies, Eugene, USA
Non-fat dry milk powder	Carl Roth, Karlsruhe, Germany
Page Ruler™ Prestained Protein Ladder	Fermentas, St. Leon-Rot, Germany
Penicillin/Streptomycin 100x	PAA Laboratories, Pasching, Austria

Phenymethylsulfonyl fluoride (PMSF)	Sigma-Aldrich, Taufkirchen, Germany
Polyacrylamide	Carl Roth, Karlsruhe, Germany
PowerUp™ SYBR® Green Master Mix	Applied Biosystems, Waltham, USA
Primers	Metabion, Planegg, Germany
Puromycin	Sigma-Aldrich, Taufkirchen, Germany
(R)-Roscovitine	Sigma-Aldrich
RNeasy® Mini Kit (250)	QIAGEN, Hilden, Germany
Sodium chloride	Carl Roth, Karlsruhe, Germany
Sodium fluoride (NaF)	Merck, Darmstadt, Germany
Sodium orthovanadate (Na$_3$VO4)	ICN, Biomedicals, Aurora, OH, USA
Sodiumdodecylsulfate (SDS)	Carl Roth, Karlsruhe, Germany
Tris Base	Sigma-Aldrich, Taufkirchen, Germany
Trypsin	PAN Biotech, Aidenbach, Germany
Tween 20	Sigma-Aldrich, Taufkirchen, Germany
William's E Medium (1X)	Life Technologies, Eugene, USA

Table 1 Reagents

3.1.2 Consumables

Product	Manufacturer
ibidiTreat µ-slides	ibidi, Martinsried, Germany
Cell culture flasks: 25 cm^2, 75 cm2	Sarstedt, Nürnbrecht, Germany
Disposable pipettes: 5 ml, 10 ml, 25 ml	Sarstedt, Nürnbrecht, Germany

Falcon tubes: 15 ml, 50 ml	Sarstedt, Nürnbrecht, Germany
Microtiter plates: 6 well, 96 well	Sarstedt, Nürnbrecht, Germany
Petri dishes: 100 mm, 40 mm	Sarstedt, Nürnbrecht, Germany
Pipette tips: 10 µl, 100 µl, 1000 µl	Sarstedt, Nürnbrecht, Germany
SafeSeal tubes: 0.5 ml, 1.5 ml, 2 ml	Sarstedt, Nürnbrecht, Germany
Nitrocellulose membrane (0.45 µM)	Amersham Bioscience, Freiburg, Germany
Polyvinylidene difluoride (PVDF) membrane (0.2 µM)	Amersham Bioscience, Freiburg Germany
Millipore Express® PLUS membrane filter (0.22 µM)	Merck Millipore, Darmstadt, Germany

Table 2 Consumable

3.1.3   Technical Equipment

Device	Producer
ChemiDoc™ Touch Imaging System	Bio-Rad Laboratories GmbH
Leica TCS SP8 confocal laser scanning microscope	Leica Microsystems
Nanodrop® Spectrophotometer	PEQLAB Biotechnologie GmbH
Orion II microplate Luminometer	Berthold Detection Systems GmbH
Primus 25 advanced® Thermocycler	PEQLAB Biotechnologie GmbH
QuantStudio™ 3 Real-Time PCR System	Applied Biosystems
SpectraFluor Plus™	Tecan

Table 3 Technical Equipment

3.1.4 Plasmids

Name	Insert	Backbone	Bac Resistance	Company
8xGTIIC-luciferase	YAP-TEAD reporter	pGL3b	Ampicillin	Addgene #34615
pGL4.34[luc2P/SRF-RE]	SRE reporter	pGL4	Ampicillin	Promega Inc.
CDK5-HA	CDK5	pCMV-neo-Bam	Ampicillin	Addgene #1872
Renilla	Luc control	n.a	Ampicillin	Addgene #2716

Table 4 Plasmids

3.1.5 Antibodies and fluorescent dyes

3.1.6 Primary antibodies

Name	Species	Catalogue	Supplier	Dilution (IF/WB/1P)
YAP (D8H1X) XP®	Rabbit IgG	14074	Cell Signaling Technology, Cambridge, UK	1:200/1:1000/-
Phospho YAP(Ser127) (D9W2I)	Rabbit IgG	13008	Cell Signaling Technology, Cambridge, UK	-/1:1000/-

LATS1 (C66B5)	Rabbit IgG	3477	Cell Signaling Technology, Cambridge, UK	-/1:1000/-
Phospho-LATS1 (Thr1079) (D57D3)	Rabbit IgG	8654	Cell Signaling Technology, Cambridge, UK	-/1:1000/-
Phospho-LATS1 (Ser909)	Rabbit IgG	9157	Cell Signaling Technology, Cambridge, UK	-/1:1000/-
TAZ (E8E9G)	Rabbit IgG	83669	Cell Signaling Technology, Cambridge, UK	-/1:1000/-
Phospho-TAZ (Ser89) (E1X9C)	Rabbit IgG	59971	Cell Signaling Technology, Cambridge, UK	-/1:1000/-
LATS2 (D83D6)	Rabbit IgG	5888	Cell Signaling Technology, Cambridge, UK	-/1:1000/-
Phospho-MST1 (Thr183)/MST(Thr180) (E7U1D)	Rabbit IgG	49332	Cell Signaling Technology, Cambridge, UK	-/1:1000/-
STK3/MST-2 (EP1466Y)	Rabbit monoclonal	ab52641	Abcam, Cambridge, UK	-/1:1000/1:50

MRTF-A (G-8)	Mouse monoclonal	Sc-390324	Santa Cruz Biotechnology, Dallas, TX, USA	1:200/-/-
CDK5 (DC34)	Mouse monoclonal	AHZ0492	Invitrogen	-/1:1000/1:50

Table 5 Primary antibodies

3.1.7 Secondary antibodies

Name	Species	Catalogue	Supplier	Dilution (IF/WB)
Alexa Fluor 488	Goat anti-rabbit IgG (H+L)	A-11008	Life Technologies, Carlsbad, CA, USA	1:400/-
Alexa Fluor HRP Conjugate	Goat anti-rabbit	7074	Cell Signaling Technology, Cambridge, UK	-/1:1000
HRP Conjugate	Goat anti-mouse	7076	Cell Signaling Technology, Cambridge, UK	-/1:1000
HRP Conjugate	Goat anti-rabbit	111-035-144	Dianova	-/1:10,000

Table 6 Secondary antibodies

3.1.8 Fluorescent dyes

Fluorescent dyes	Company
Hoechst 33342	Sigma Aldrich, St. Louis, MO, USA
Rhodamin-phalloidin	Sigma Aldrich, St. Louis, MO, USA
Cell tracker green bodipy	Thermo Fisher Scientific,USA

Table 7 Fluorescent dyes

3.1.9 Software

Software	Origin
GraphPad Prism 9	GraphPad Software, San Diego, CA, USA
ImageJ	National Institutes of Health, Behtesda, MD, USA
ImageJ plugin Nuclei Cytoplasm	FAIR Data Informatics Lab, University of California, San Diego, CA, USA
Bio-Rad Image Lab Software	California, USA
Microsoft Office Standard	Microsoft, Redmond, WA, USA

Table 8 Softwares

3.2 Cell culture

3.2.1 Cell culture buffers and solutions

PBS (pH 7.4)		Trypsin/EDTA (T/E)	
NaCl	132.2 mM	Trypsin	0.05 %
Na_2HPO_4	10.4 mM	EDTA	0.02 %
KH_2PO_4	3.2 mM	PBS	
H_2O			

PBS+Ca^{2+}/Mg^{2+} (pH 7.4)		Freezing medium (Huh7 cells)	
NaCl	137 mM	DMEM	70%
KCl	2.68 mM	FCS	50 mL
Na_2HPO_4	8.10 mM	DMSO	10%
KH_2PO_4	1.47 mM		
$MgCl_2$	0.25 mM		
H_2O			

Growth medium		Collagen G	
DMEM	500 mL	Collagen G	0.001%
FCS	50 mL		
Puromycin	1 µg/µL	PBS	5 mL

Table 9 Cell buffers and solutions

3.2.2 Creation of Huh7 nt and Huh7 CDK5 KD cell lines with stable CDK5 knockdown expression

For the creation of Huh7 nt cells and Huh7 CDK5 KD cells, transduction of Huh7 cells was carried out with Cdk5 shRNA and nt shRNA Cdk5 MISSION® shRNA Lentiviral Transduction Particles (Vector: pLKO.1-puro; SHCLNVNM_ 004935; Clone ID: (1) TRCN0000021465, (2) TRCN0000021466, (3) TRCN0000021467, (4) TRCN0000194974, (5) TRCN0000195513; Sigma-Aldrich) and MISSION® pLKO.1-puro Non-Mammalian shRNA Control Transduction Particles (SHC002V; Sigma-Aldrich) as a control were used according to the manufacturer's protocol. Both cell lines were transduced with a multiplicity of infection (MOI) of one and

successfully transduced cells were selected by adding 2µg/ml puromycin to the medium. Puromycin concentration was reduced to 1µg/mL after initial selection to ensure stable transfection with CDK5 shRNA and ntRNA. After the initial selection, puromycin concentration was reduced to 1µg/mL for further cultivation to ensure stable transfection with Cdk5 and nt shRNA. The most efficient and well-tolerated clones were selected through Western Blot analysis [70].

3.2.3   Cell Culture

Successfully transduced Huh7 nt and Huh7 CDK5 KD cells were cultured with high glucose DMEM supplemented with 10% FCS (PAN Biotech GmbH) and Puromycin (50 uL/mL) and cultivated at 37 degrees under 5% CO_2 atmosphere. Before passing and seeding of cells all the culture flasks, multiwall plates and dishes were coated with collagen G (0.001% in PBS, Sigma Aldrich)

3.2.4   Passaging

When cells reached confluency, they were either subcultured 1:2 – 1:10 in 75 cm^2 culture flasks or seeded in multiwall plates and dishes for further experiments. For the detachment of cells, they were washed with prewarmed PBS followed by brief incubation with trypsin for 2-3 mins at 37°CTrypsin digestion was stopped by adding a growth medium. To prepare the cells for platting, trypsin was removed by centrifugation and then the fresh medium was added. After that cells were counted using the vi-cell counter.

3.2.5   Freezing and thawing

For long-term storage, cells were detached as described previously and resuspended in an ice-cold freezing medium which contained 20% FCS and 10% DMSO. Aliquots of 1.5 ml were transferred to cryovials. Cells were then initially stored at -80°C for 24h, then the cryovials were moved to liquid nitrogen for long-term storage. For thawing, cryovials were initially warmed to 37°C and then cell culture medium was immediately added to the cell suspension. Through centrifugation (1000 rpm, 5 min, 20°C) excessive DMSO was removed by replacing the freezing medium with fresh growth medium.

3.3 Transfections and Plasmids

Luciferase reporter constructs pGL4.74 (renilla control) and pGL4.34 (SRE-SRF,) were purchased from Promega (Madison, WI, USA), and the 8xGTTIC YAP/TAZ firefly construct was from Add gene (RRID: Addgene_34615). Huh7 nt cells were transfected using Lipofectamine 3000 transfection kit (Thermofisher) according to manufacturer instructions. For reporter gene assay, Fugene transfection reagent (Promega) was used to perform transfection according to the manufacturer's protocol. Western blot and immunostaining were performed between 24h and 48h after transfection.

3.4 Luciferase reporter gene assays

An Orion II microplate luminometer equipped with Simplicity Software (Berthold Detection Systems GmbH, Germany) was used to perform Luciferase reporter gene assays. Initially, cells (seeding density of 1×10^6 cells/well) were transfected with YAP and Renilla Luciferase reporters using Fugene transfection reagent for 24h in 6 well plates. Later the next day cells were reseeded in 24 well plates and stimulated with thrombin for 1h. Firefly and Renilla vectors were used in a ratio of 10:1. Finally, Firefly/Renilla luciferase intensity levels were determined with the Dual-Luciferase® Reporter Assay kit by Promega (Madison, WI, USA). MRTF activity was also determined by SRF Luc reporter by the same method.

3.5 Immunostaining

All the staining experiments were performed in Ibitreat ® 8 well µ-slides from Ibidi (Gräfelfing, Germany). For immunofluorescence staining, cells were washed with PBS+ and fixed with 4% paraformaldehyde in PBS for 10 min. After washing with PBS, cells were incubated in 0.1% Triton $\times$-100 in PBS for 10 min for membrane permeabilization. After another brief washing step, cells were incubated in 1% BSA in PBS for 1h at room temperature for blocking of unspecific binding sites. After blocking, cells were incubated with primary antibody diluted in 0.2% BSA in PBS (1:200) overnight at 4 °C. Next day slides were then washed with 3 x 10 min with 1 % BSA in PBS and then incubated in secondary antibody (1:400) and Hoechst

33342 (1:100) for nuclear counter stain in PBS for 1h at RT. Finally, cells were washed for 2 x 10 min with 1 % BSA in PBS and once with PBS for 10 min. Slides were sealed with FluorSave Reagent (Merck, Darmstadt, Germany), and stored at 4 °C in the dark.

3.6   Laser scanning confocal microscopy

Confocal images were acquired with a Leica TCS SP8 SMD confocal microscope, equipped with an HC PL APO 63x/1.40 oil objective and photomultiplier (PMT) or HyD detectors. Pinhole size was adjusted to 1.0 airy units and sequential scanning was performed with a scanning speed of 400 Hz. Following excitation laser lines were applied: 405 nm, 488 nm, and 647 nm.

3.7   Analysis, Calculation of nucleus to cytoplasm ratio

For the calculation of the nucleus-to-cytoplasm ratio, the nucleus-to-cytoplasm intensity tool from Fiji was employed (Intensity Ratio Nuclei Cytoplasm Tool, RRID:SCR_018573) For every repetition 10 images were evaluated, and 3 repetitions were done. In each image there were about 70-80 cells which were evaluated by the plugin. Later quantifications were made using Plugin and unpaired t test was employed followed by Welches correction was employed, and later p value was determined.

3.8 Western Blot

3.8.1 Western Blot buffers

RIPA lysis buffer	
Tris/HCl	50 mM
NaCl	150 mM
Nonidet NP-40	1 %
Sodium deoxycholate	0.25 %
SDS	0.10 %
H_2O	
Additional inhibitors (per100 mL of RIPA buffer)	
β-glycerophosphate	3mM
Na_2VO_3	300 µM
NaF	1mM
$Na_4P_2O_7$	10mM
added before use:	
Complete®EDTAfree	4 mM
PMSF	0.5 mM
activated Na_3VO_4	2 mM

Separation gel 6-12%	
Rotiophorese™ Gel 30	40 - 80 %
Tris (pH 8.8)	375 mM
SDS	0.1 %
TEMED	0.1 %
APS	0.05 %

5X SDS sample buffer	
Tris/HCl pH 6.8	3.125 M
Glycerol	50 %
SDS	5 %
DTT	2 %
Pryonin Y	0.025 %
H_2O	

Electrophoresis buffer	
Tris	4.9 mM
Glycine	38 mM
SDS	0.1 %
H_2O	

TBS-T (pH 7.6)	
Tris/HCl	50 mM
NaCl	150 mM
Tween 20	0.05 %

Tank buffer	
Tri's base	48 mM
Glycine	39 mM
Methanol	20 %
H_2O	

Stacking gel	
Rotiophorese™ Gel 30	17 %

Tris (pH 6.8)	125 mM
SDS	0.1 %
TEMED	0.2 %
APS	0.1 %
H_2O	

Table 10 Western blot buffers and reagents

3.8.2 Cell lysis and total protein isolation

Cells were washed with ice-cold PBS 2x times. After that cold RIPA plus lysis buffer with added inhibitors was added. Cell lysates were stored at -80°C for at least 1h or overnight. After thawing, the cells were scraped off with a cell scraper and the resulting residual was transferred to 1.5 mL tubes. After centrifugation (14000 rpm, 4°C, 10 min), the pellet was discarded. Protein concentration was determined by Bradford assay. All samples were diluted to 1:10 and absorbance was detected at 592 nm using SpectraFluor Plus™. The final protein concentration was determined by plotting a standard BSA linear standard dilution curve. All the cell lysates were then prepared accordingly by diluting them with 5X sample buffer and were stored at -20°C until further western blot analysis.

3.8.3 Sodium Dodecyl Sulfate Polyacrylamide Gel Electrophoresis (SDS-PAGE) and Immunoblotting

Protein separation was performed using SDS PAGE electrophoresis (80V, 90min, RT) and subsequent transfer to nitrocellulose membranes (0.25-micron pore size) (100V, 1.5h, RT). After that, membranes were incubated in blocking solution (5% BSA in TBS-T & 5% Blotto in TBS-T) for 2h at RT followed by incubation in primary antibodies overnight at 4°C. Subsequently, membranes were washed 3 times with 1× TBS-T for 5 min each. Then the membranes were incubated in secondary antibody for 2h followed by 4 washing steps with TBS-T, 5 min each. After that chemiluminescence was detected by incubating the membranes with ECL solution and 2.5 mM luminol. HRP conjugated proteins were detected by ChemiDoc™ Touch Imaging System (Bio-Rad) and the bands were identified by comparing with Page Ruler™ Plus Prestained Protein Ladder. Normalization of protein loading was performed using the Image Lab™ Software (Bio-Rad).

3.9   Co-immunoprecipitation

For Co-IP experiments, cells were first rinsed 3x with ice-cold PBS and then pre-cooled RIPA lysis buffer was added. After that, the cells were stored at -80°C for at least 1h or overnight. Cells were scrapped off with a cell scraper and the resulting residual was transferred to 1.5 mL tubes. The lysates were recovered after centrifugation and the protein concentration was determined using the Bradford assay. All steps were performed on ice.

Afterwards, 2 μg of monoclonal antibody and 50 μL of μMACS Protein G MicroBeads were added to the lysates. The lysates were then incubated at 4°C overnight with shaking. The next day the conjugated protein was recovered by magnetic separation under a strong magnetic field using a magnetic μMACS Column. After incubation with the protein solution, the column was rinsed 3x with RIPA buffer and 1x with low salt buffer. After that, the column was rinsed with pre-boiled 20 μL SDA PAGE sample buffer and incubated for 5 mins. Later the protein was eluted in fresh 1.5 mL tubes by applying 50 μL pre-boiled sample buffer. Eventually, the protein concentration was adjusted by adding SDA PAGE sample buffer and the samples were boiled for 5 min at 95°C and stored at -20°C and then subsequent western blot was done.

3.10   Quantitative Real-time PCR (qPCR)

The mRNA was isolated by QIAGEN RNeasy Mini kit according to manufacturer protocol and was reversely transcribed to cDNA by a High-capacity cDNA Reverse Transcription kit, Applied Biosystem. After that qPCR was performed with GAPDH serving as the housekeeping gene as described previously[71] .Primers were purchased from Metabion and the sequences of primers used for qPCR analysis are listed in the table(11)

Target	Forward Sequence	Reverse Sequence
CTGF	5'-TGGAGTTCAAGTGCCCTGAC-3'	5'-CTCCCACTGCTCCTAAAGCC-3'

| CYR 61 | 5'-ACCCTTCTCCACTTGACCAG-3' | 5'-CTTGGCGCAGACCTTACAG-3' |
| GAPDH | 5'-ACGGGAAGCTTGTCATCAAT-3' | 5'-CATCGCCCCACTTGATTTT-3 |

Table 11 qPCR primers

3.11 Spheroids

3.11.1 Spheroid culture

Spheroids were formed using hanging drop method. Each drop comprised of 1000 cells and total cell density was 50,000 cells/ml used with 20% methocel stock solution with cell culture medium. Drops were pipetted out to the lid of 100 mm petri dish and then incubated overnight where spheroids were allowed to form.

Next day spheroids were harvested in PBS by centrifugation at RT at 1000 rpm for 5 mins and resuspended in mixture of collagen solution. After that the spheroid collagen solution was seeded on the collagen gel coated ibidi slides in varying volumes and again incubated to polymerise for 30 mins followed by addition of cell culture media. Next day spheroids were visualised in bright field microscope.

3.11.2 Collagen Gel formation

Ibidi collagen was used and prepared as per manufacturer protocols and 75 µl of it was seeded per well of Ibidi well and incubated in incubator for 30 mins and left to polymerize. After that next layer of collagen containing spheroids was embedded on the top and left again top polymerase for 30 mins in the incubator.100 µl of cell culture media was added and then the slides were kept in incubator. Next day spheroids were visualised in bright field microscope.

3.11.3 Immunostaining of spheroids

Spheroids were fixed with PFA 4% for 30 mins and then washed with PBS for 10 mins followed a membrane permeabilization with 0.2% triton-X for 30 mins. Next the slides were washed again with PBS for 10 mins and blocked with 1% BSA in PBS for10 mins. Next the slides were incubated with primary antibody overnight at 4°C and next day washed.

3.12 Phosphoproteomics

3.12.1 Materials

Solvents and Reagents	Producer
Acetonitrile	LC-MS Merck, Darmstadt, Germany
Ammonium hydrogen carbonate	Roth, Karlsruhe, Germany
Dithiothreitol (DTT)	Roth, Karlsruhe, Germany
Formic acid (FA)	Merck, Darmstadt, Germany
Endopeptidase Lys-C, MS grade	Fujifilm Wako Chemicals, Richmond, USA
Pierce 660 nm Protein Assay Reagent	Thermo Fisher Scientific, Waltham, USA
Tris-(2-carboxyethyl)-phosphine (TCEP)	Roth, Karlsruhe, Germany
Trypsin, modified, sequencing grade	Promega, Madison, USA
Trypsin / Lys-C Mix, mass spec grade	Promega, Madison, USA
Promega, Madison, USA	Karlsruhe, Germany
Water, LC-MS grade	Darmstadt, Germany

Table 12 Solvents and reagents for phosphoproteomics

Equipment	Manufacturer
Centrifuge 5427 R	Eppendorf, Köln, Germany
Q Exactive HF-X mass spectrometer	Thermo Fisher Scientific, Waltham, USA

Thermomixer 5436	Eppendorf, Köln, Germany
Ultimate 3000 RSLC System	nano System Thermo Fisher Scientific, Waltham, USA
5600+ mass spectrometer	Sciex, Concord, Canada
Ultrasonicator Sonopuls UW3200	Bandelin, Berlin, Germany
Vacuum concentrator	Bachofer, Reutlingen, Germany

Table 13 Equipments for Phosphoproteomics

Plasticware	Manufacturer
Amicon Ultra 2 mL Centrifugal Filters (3K)	Merck, Darmstadt, Germany
Amicon® Ultra 0.5 mL Centrifugal Filters (3K)	Merck, Darmstadt, Germany
QIAshredder	QIAGEN, Hilden, Germany
Safe-Lock Tubes (1.5 mL & 2 mL)	Eppendorf, Köln, Germany

Table 14 Consumbables for Phosphoproteomics

3.12.2 Sample Preparation

For phosphoproteomics cells were initially seeded on 6 well dishes (1 * 10^6 cells/well) After they were trypsinised and thoroughly washed with 5X with PBS to remove any residues for FCS and cell culture media. After that samples were lysed in 60 µL with 8M Urea/0.4 M NH_4HCO_3 using a sonicator followed by a reduction at 37°C with DTT for 30 mins. After that, alkylation with 0.1 M iodoacetamide in the dark at RT was carried out. Then, a first digestion was done using LysC (1:100, enzyme: protein) at 37°C for 4h. Next, the samples were diluted in 1M urea with water followed by a trypsin digestion (1:50 protein to trypsin ratio) at 37°C overnight. Followed by this, acidification was done with formic acid. Next phosphor enrichment was carried out with High Select™ Phosphopeptide Enrichment Kits & Reagents (#A32993). from Thermofisher Scientific as per manufacturer protocols.

3.12.3 LC method

For the whole proteome, peptides were separated with an EASY-Spray column (PepMap RSLC C18, 75 μm × 50 cm, 2 μm particles, ThermoScientific) at a flow rate of 250 nL/min using a two-step gradient: Starting with 3 % B to 25 % B in 160 min, followed by a 10 min ramp to 40 % B (A: 0.1% formic acid in water, B: 0.1 % formic acid in acetonitrile). For the phosphoproteome, using the same eluents, the gradient started from 3 % to 25 % B in 30 min, followed by ramping to 40 % B in 5 min.

3.12.4 MS method

LC was coupled to a Q Exactive HF-X mass spectrometer (Thermo Scientific), which was run in the data-dependent acquisition mode with a maximum of 15 MS/MS spectra per survey scan for the analysis of cell lysates and testicular tissue. For the phosphoproteome a maximum of 5 MS/MS spectra was used. Survey scans were measured with a resolution of 60,000 at 200 m/z and product ion spectra were produced with collision induced dissociation and analyzed with a Resolution of 15,000 at 200 m/z.

3.12.5 Data analysis

Raw spectra files from both the full proteome and phosphoproteome samples were searched together using MaxQuant (v. 2.0.3.0) [72] using all human entries from Swissport and the standard contaminant database. The PTM and match between runs features were turned on. False discovery rate (FDR) was controlled to be 1 %. Statistical evaluation and analysis were done using Perseus (v. 1.6.5.0) [73] and R[74]. The data were $\log_2$ transformed and normalized by using mean centering of the values in each sample of 5 replicates. Fold change and q values between KD and NT groups were calculated and volcano plots were generated after performing Welch's T-test and at FDR 5%. Phosphosite plus was used for further phosphoproteome analysis. In order to determine a significant quantitative difference in terms of the changes a set of criteria was set in terms of q values and $\log_2$ fold change.

3.13 Yeast two Hybrid System

3.13.1 Materials

Materials	Company
Dimethylsulfoxide (DMSO)	VWR, Ismaning, Germany
Hydrochloric acid (HCl)	VWR, Ismaning, Germany
Sodium hydroxide (NaOH)	VWR, Ismaning, Germany
Ultra-pure water (18MΩ.cm [1])	Millipore S.A.S. Milli-Q Academic system, Molsheim, France
Ammonium acetate (NH$_4$AcO)	Merck KGaA, Ismaning, Germany
Bovine serum albumin (BSA)	Merck KGaA Ismaning, Germany
Calcium chloride (CaCl$_2$)	Merck KGaA, Ismaning, Germany
Sorbitol	Merck KGaA, Ismaning, Germany
Magnesium chloride (MgCl$_2$)	AppliChem, Darmstadt, Germany
Glycerol	AppliChem, Darmstadt, Germany
Agar-Agar	Carl Roth, Karlsruhe, Germany
Ampicillin	Carl Roth, Karlsruhe, Germany
Potassium chloride (KCl)	Carl Roth, Karlsruhe, Germany
Sodium dodecyl sulfate (SDS)	Carl Roth, Karlsruhe, Germany
Lithium acetate	BioScience,GmbH,Dümmer, Germany
Yeast nitrogen base	Sigma-Aldrich, Taufkirchen, Germany
PEG	Takara Bio

Yeast synthetic drop-out medium	Sigma-Aldrich, Taufkirchen, Germany
Yeast supplements	Sigma-Aldrich, Taufkirchen, Germany
Adenine	Sigma-Aldrich, Taufkirchen, Germany
Tryptophan	Sigma-Aldrich, Taufkirchen, Germany
Potassium phosphate dibasic (K_2HPO_4)	Sigma-Aldrich, Taufkirchen, Germany
Potassium phosphate monobasic (KH_2PO_4)	Sigma-Aldrich, Taufkirchen, Germany
Magnesium sulfate ($MgSO_4$)	Sigma-Aldrich, Taufkirchen, Germany
Tris-HCl	Sigma-Aldrich, Taufkirchen, Germany
HEPES	Sigma-Aldrich, Taufkirchen, Germany
Sodium chloride (NaCl)	Sigma-Aldrich, Taufkirchen, Germany
Matchmaker® Gold Yeast two-hybrid System	Takara Bio
Yeast Media Set 2 Plus	Takara Bio
Matchmaker® Insert Check PCR Mix 2	Takara Bio
Easy Yeast Plasmid Isolation Kit	Takara Bio
Mate&Plate™Library – Universal Human	Takara Bio

Table 15 Materials yeast two hybrid

3.13.2 Cloning Procedure

CDK5 was amplified from a CDK5 containing plasmid for mammalian expression (Plasmid 1870, addgene) using the following primers adding BamHI and EcoRI restriction sites:

Forward primer: 5'-C ATG GAG GCC GAATTC ATG CAG AAA TAC GAG AAA CTG GAA-3'.

Reverse primer: 5'-GC AGGTCGACGGATCC GGA TCC GGG CGG ACA GAA GTC GGA-3'.

The PCR products were analyzed by a 1% agarose gel and purified using a gel extraction kit (Qiagen). The purified insert and the bait vector pGBKT7 (Takara Bio) were digested with BamHI and EcoRI (Thermo Fisher Scientific); lower concentrations than indicated in the protocol were used for EcoRI and CDK5, since CDK5 contains a restriction site for EcoRI. The vector was further dephosphorylated by directly adding 1 µL of FastAP Thermosensitive Alkaline Phosphatase (Thermo Scientific). Vector and insert were again purified using a gel extraction kit. Ligation (was carried out in a 1:3 ratio (vector: insert) using the protocol from Thermo Fisher Scientific at room temperature for 30 min, followed by heat shock transformation of the ligation mixture into chemical competent *E. coli* DH5-α. Plasmid isolation was performed using the QIAprep® Spin Miniprep Kit (Qiagen). Plasmids were analyzed by PCR and sequencing using a standard T7 primer (Eurofins).

3.13.3 Method

The Matchmaker Gold yeast two hybrid system (Takara Bio) was used to screen for interaction partners of CDK5 following the manufacturer's instructions. In brief, CDK5 was amplified from pCMV neo with primers adding restrictions sites for BamHI and EcoRI, and subsequently cloned into the pGBKT7 bait vector. The vector was introduced int the Y2H Gold reporter strain, which was then mated with the Mate&Plate™ library – Universal Human (normalized) (Takara Bio) in yeast strain Y187. The mating efficiency was calculated as 10.1% by plating serial dilutions. The screening was performed following the Matchmaker manual. An aliquot of 4.7×10^7 cfu was screened (15-fold library coverage) on 4 plates (15 cm diameter) containing DDO/X/A medium. After incubation, 316 blue colonies were picked from the 4 plates, and respotted on DDO/X/A and QDO/X/A plates, respectively. Colonies which showed robust growth and blue colour on both plates

were classified as 'hits', and colony PCR was performed for those colonies. Samples showing a band on an agarose gel were analysed by sequencing (152 samples, Eurofins Genomics, T7 standard sequencing primer) (Supplementary table 16). STK3 was identified 36 times. One colony containing the STK3 hit was selected, and the plasmid was isolated (Easy Yeast Plasmid Isolation Kit, Clontech), amplified in E. coli, and re-transformed into the Y2H Gold reporter strain already containing the CDK5 bait plasmid. As control, the reporter strain containing the CDK5 bait plasmid was transformed with an empty bait vector not carrying any insert. A prey rescue experiment was performed (Figure 1), confirming the interaction between CDK5 and STK3.

RESULTS

4 Results

4.1 MST2 is an interacting partner of CDK5

The project started when Prof. Dr. Simone Moser (Pharmaceutical Biology, Department of Pharmacy, LMU Munich) performed yeast two hybrid screening which confirmed the interaction between STK3 and CDK5. STK3 was determined as one of the major hits and was identified 36 times in Yeast matchmaker experiment. After that prey rescue experiment also finally confirmed STK3 as an interacting partner for CDK5 (Figure 8A-C)

Next to substantiate this interaction further co-immunoprecipitation experiments were conducted, where either a CDK5 antibody was utilised for IP and presence of STK3 was observed *via* Western blot, and *vice versa*. Bands of STK3 and CDK5 were observed at 75 kDa and 35 kDa respectively validating the interaction between CDK5 and STK3 (Figure: 8D E).
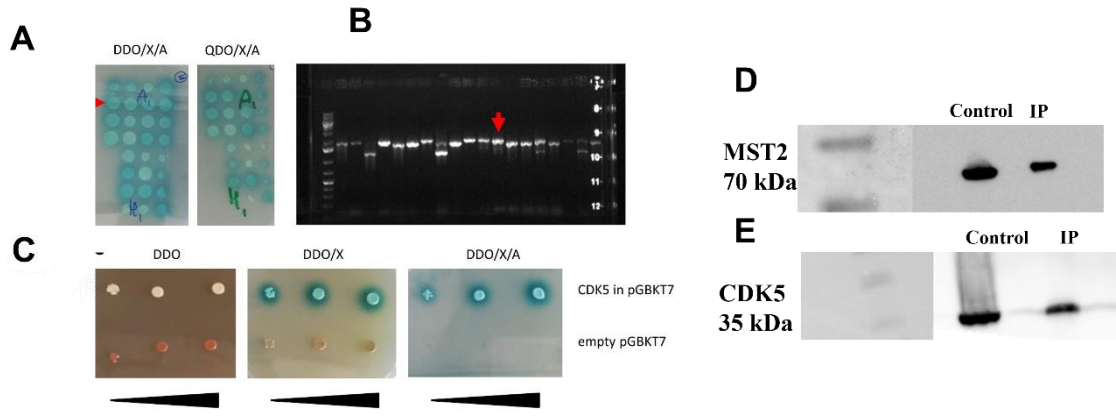
Figure 8 MST2 is an interaction partner of CDK5. (A) Y2H screening of CDK5. The screening was performed using DDO/X/A as selective medium. 316 blue colonies were obtained, which were re-spotted onto selective plates with increasing stringency (DDO/X/A and QDO/X/A, example shown in panel A). Only colonies, which showed robust growth on both plates, were selected, colony PCR was performed (B), and samples were analyzed by Sanger sequencing. Of the 36 colonies containing a plasmid with the insert encoding for STK3, one colony was selected (marked with a red arrow in A and B). The plasmid was isolated, and a prey rescue experiment was performed (C): The prey plasmid with the STK3 insert and the empty prey plasmid were re-transformed into the Y2H gold reporter strain with the CDK5 bait plasmid. A Y2H spot test was performed, in which the two strains (empty prey plasmid and prey plasmid with CDK5 insert) were spotted DDO plates (confirmation of prey and bait plasmid being present), and two selective plates (DDO/X gives blue colonies if an interaction takes place but the yeast can also grow without the interaction, and DDO/X/A plates, on which the yeast can only grow if an interaction takes place). The prey rescue experiment clearly confirms the interaction between CDK5 and STK3 in the Y2H setup. Black triangles represent serial dilutions. (D and E) Co-immunoprecipitation experiments confirming this interaction (D) CDK5 antibody was utilised for IP and blotted for MST2 (STK3) (70 kDa), (E) MST2 (STK3) antibody was utilised for IP and blotted for CDK5 (35 kDa), experiments were done in triplicates to confirm this interaction, control lane referring to bead controls and IP lane referring to immunoprecipitation lane.

4.2 CDK5 knockdown reduces YAP reporter activity.

To investigate potential functional consequences of the interaction between MST2 (STK3) and CDK5, we analysed YAP activity changes after CDK5 knockdown. For this we performed a reporter gene assay with Huh7 control cells (treated with non-targeting shRNA), and Huh7 CDK5 KD clones.

Interestingly, we found that Huh7 CDK5 KD clones have reduced YAP reporter activity (almost by half) as compared to Huh7 nt control cells (Figure 9A). We also treated the cells with thrombin for 30 min to stimulate and activate YAP so that it translocates back to the nucleus. Thrombin treatment was used as a positive control for active YAP. Thrombin is a serine protease activator, which activates the Protease-activated receptors, and consequently YAP by decreasing

phosphorylation and increasing nuclear localisation [75]. In the case of thrombin treatment, reporter activity of YAP increases as expected in both Huh7 CDK5 KD clones and Huh7 nt control cells. However, still there was a difference in the reporter activity where thrombin treated Huh7 CDK5 KD clones exhibited reduced YAP activity as compared to control (Figure 9A).

To obtain a global view of how exactly CDK5 is involved in the Hippo pathway, we decided to work with CDK5 overexpressing cells as well. We transfected Huh7 nt control clones with CDK5 overexpressing plasmid (Huh7 CDK5 Overexpressing cells). After 48h the transfection efficiency was maximum as most of the CDK5 was expressed by the cells (Supplementary Figure 18). Therefore, we decided to keep this time point for all our further experiments.

It has been widely accepted that cell confluence regulates several signalling pathways and affects the tensional status of cells. Proteins are sensitive to cell density-mediated nucleo-cytoplasmic shuttling. YAP is one such protein which exhibits cell density mediated nucleo-cytoplasmic shutting. To understand the behaviour of YAP concerning cell density and to establish the least conditions of intracellular YAP activation, immunostaining experiments were performed on Huh7nt, Huh7 CDK5 KD cells and Huh7 CDK5 overexpressing cells keeping high cell density. The cells were also treated with thrombin for 30 min. In all the groups with thrombin stimulation compared to the groups without thrombin treatment, the ratio of nuclear to cytoplasmic YAP intensity was calculated as readout. Most of the YAP got activated and translocated into the nucleus upon treatment of the cells with thrombin in all three groups. As was to be expected after the reporter gene results, overall YAP activity was lower in the CDK5 KD cells. Astonishingly, overexpression of CDK5 made no difference concerning activation of YAP (Figure 9B1-3, C).

We next looked for the expression of total YAP and its degree of phosphorylation using Western blot analysis in all three cell groups (Huh7 nt control clones, Huh7 CDK5 KD clones and Huh7 CDK5 overexpressing cells (Figure 9D, E). The total YAP levels did not seem to vary in all three groups, but it was interesting to find that in Huh7 CDK5 KD clones have higher levels of phospho YAP almost 2-fold

compared to Huh7 control clones (Figure 9F, G). These results were in conjugation with reporter gene assay and the staining results, as in the phosphorylated state, YAP is inactive and hence exhibits less activity. Only when activated, it gets translocated into the nucleus. Phospho levels of YAP are inversely related to its reporter activity. Overexpressing cells also exhibited higher levels of phospho YAP which was interesting as well (Figure 9F, G). It seemed that both CDK5 knockdown and overexpression have influenced the levels of phosphorylated YAP. This data points to the fact that CDK5 is involved in regulating the overall behaviour of YAP in the hippo pathway.
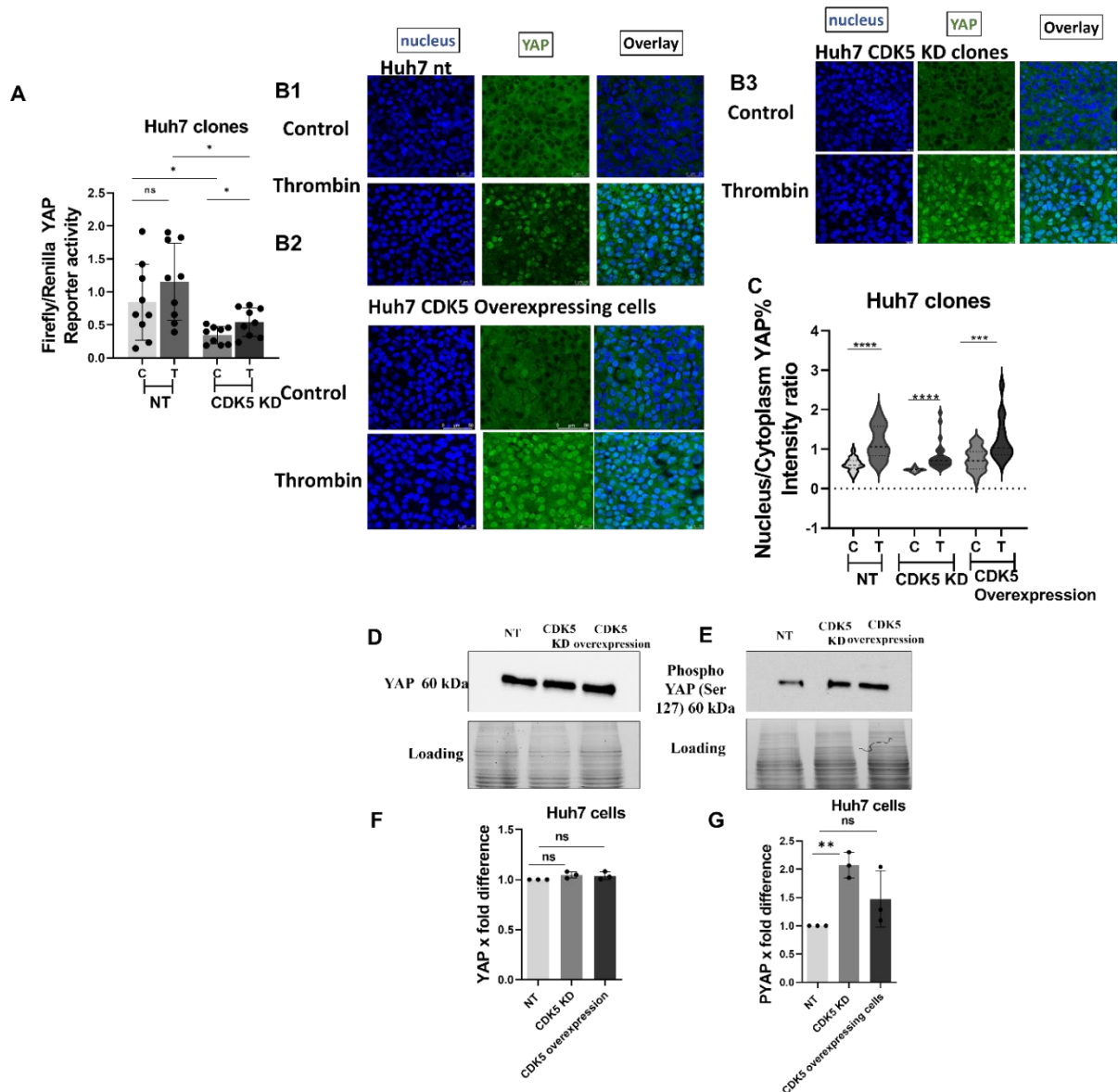
Figure 9 CDK5 knockdown reduces YAP reporter activity. (A) Dual luciferase reporter gene assay for TAED 8xGTIIC- response element comparing the YAP reporter activity of Huh7 nt controls cells (NT) and Huh7 CDK5 Knockdown clones (CDK5 KD) with (T) and without (C) 0.5U Thrombin stimulation, Luciferase reporter activity is expressed as firefly RLU normalised to the constitutive renilla control construct. (mean ± SEM for three independent experiments, unpaired t-test followed by Welches correction, *P < 0.05, ns, not significant).(B 1-3) Immunostaining of YAP on Huh7 nt control cells, Huh7 CDK5 knockdown clones and Huh7 CDK5 overexpressing cells seeded on plastic dishes with high cell density, 2* 105 cells/well, with and without thrombin stimulation, (0.5U, 30 min).(C) Nucleus to cytoplasm YAP intensity ratio analysed with the Intensity Ratio Nuclei Cytoplasm Tool plugin for Fiji ImageJ software and presented as bar graph (mean ± SEM for 3 independent experiments with 10 images per experiment, unpaired t-test followed by Welches correction, ***P < 0.05, ****P < 0.0001)(D&E) Western blot for YAP and phosphor YAP (Ser 127) in Huh7 nt control cells (NT), Huh7 CDK5 knockdown clones (Huh7 CDK5 KD) and Huh7 CDK5 overexpressing, (E&F) Qualitative expression of protein levels from, (F&G) is shown (mean ± SEM for three independent experiments, one-way ANOVA followed by Dunnett's multiple comparison test, ns, not significant).

4.3   CDK5 influences the phosphorylation levels of kinases involved in Hippo pathway kinases.

Next, to shed a clear light on the picture we decided to look for the expression of all upstream and downstream Hippo pathway kinases. We checked the expression of total protein as well as the phosphoprotein levels of the following kinases in all the three cell groups with and without thrombin stimulation

Three cell groups: - Huh7 nt control cells, Huh7 CDK5 KD clones, Huh7 CDK5 Overexpressing cells (Figure 10C).

Hippo pathway factors

Upstream kinases: -

STK3/pMST1 (Thr 183).MST2(Thr 180), LATS1/pLATS1(Thr 1079), LATS2, pLATS1(Ser 909)

Downstream kinases/Oncoproteins: - YAP/pYAP (Ser 127), TAZ/pTAZ (Ser 89)

For this it was very important to determine the time point at which after thrombin treatment YAP was completely activated and that its phospho levels were negligible. For this, we did a western blot on Huh nt control clones and after 1h YAP seem to be most activated. We decided to keep the thrombin treatment time point at 15 min for the western blot for upstream kinases and 1h for downstream kinases (Figure 10A, B). The ratio of Phosho protein to total protein was calculated as a readout to determine how much protein was phosphorylated. All the values were normalised compared to Huh7 nt control cells intensity values.

We observed that the expression level of total protein in all three cell groups of both upstream and downstream kinases did not seem to vary at all (Figure 11 A-E) and remained the same as expected. Expression of phospho MST1/MST2 did not seem to change as well and the ratio of phospho levels of protein to total protein remained almost the same in all the groups. (Figure 11A,11F). Interestingly, however, there was a significant increase in phospho LATS1 (Thr 1079) in the case of the CDK5 Knockdown and CDK5 overexpressing group (Figure 11B). This could

mean that more LATS1 is phosphorylated at Thr 1079 and there was a remarkable increase in the ratio of phosphorylated to total protein almost 2-fold times in the CDK5 knockdown group and as well as the CDK5 overexpressing group. (Figure 11G). However, there were no significant changes in the expression levels of phospho LATS1 at a different phosphorylation site (Ser 909) (Figure 11H). Upon treatment with thrombin, there was an activation of the kinase cascade and the levels of phospho LATS1 (Thr 1079) dropped as expected in all the 3 groups. (Figure 11G).

Coming more to the downstream of the hippo pathway kinases, the total expression of oncoproteins, YAP and TAZ did not seem to vary at all (Figure 11D, E). Nevertheless, the phospho levels of YAP in the case of CDK5 knockdown and CDK5 overexpression were more (Figure 11D). The ratio of phosphorylated YAP to total YAP was calculated and later the values were normalised with control. There was about a 2-fold change in the levels of phospho YAP (Figure 11J) for Huh7 CDK5 KD clones. More YAP got activated and the phospho levels diminished upon thrombin stimulation (Figure 11J). The levels of phospho TAZ in the case of CDK5 knockdown did not vary much as compared to CDK5 overexpression which seemed to get varied up to a certain extent (Figure 11E). However, upon thrombin treatment, the phospho level of TAZ was reduced. The ratio of phospho TAZ to total TAZ was determined for all the groups compared to control. For all the groups pTAZ/TAZ ratio changed upon thrombin treatment. (Figure 11K)

The increased levels of phospho LATS1 (Thr 1079) with CDK5 knockdown and overexpression seem to further influence and regulate the expression of downstream kinase/oncoprotein too, especially of YAP. The more phosphorylated LATS1(Thr 1079), the more phosphorylated YAP is, and hence the lower its activity. Overall, we determined that CDK5 has a significant influence on the overall phospho levels of LATS1 and YAP.
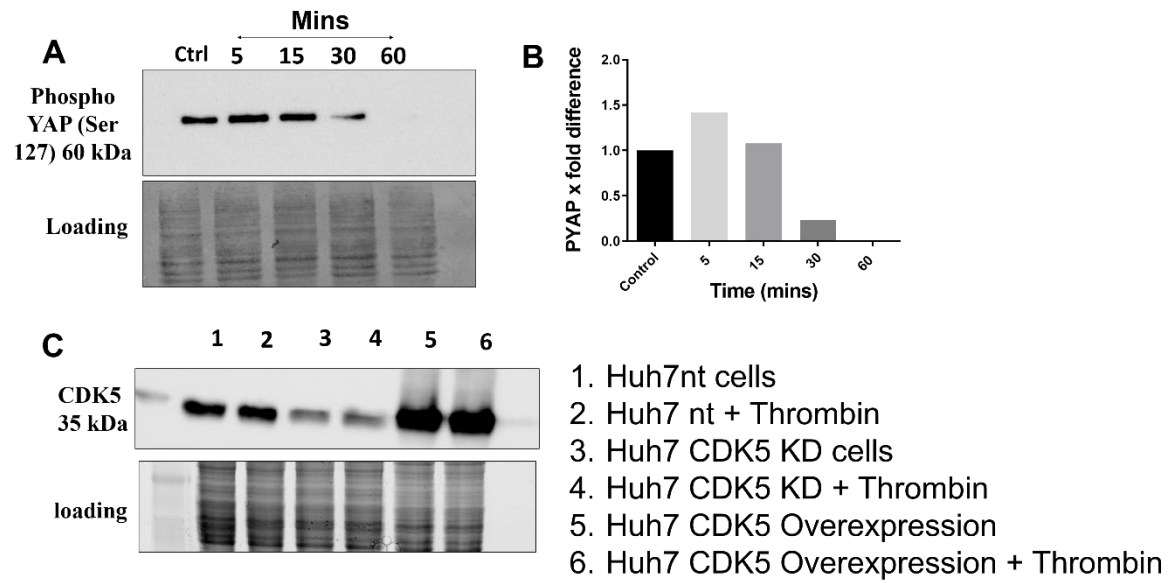
Figure 10 Thrombin treatment. (A) Huh7 nt cells were treated with thrombin and phospho YAP expression was looked over time to establish the time point at which most of the YAP is activated and phospho levels diminish, (B) Quantification of pYAP levels over the period (C) Western blot expression for CDK5 in all the three groups.
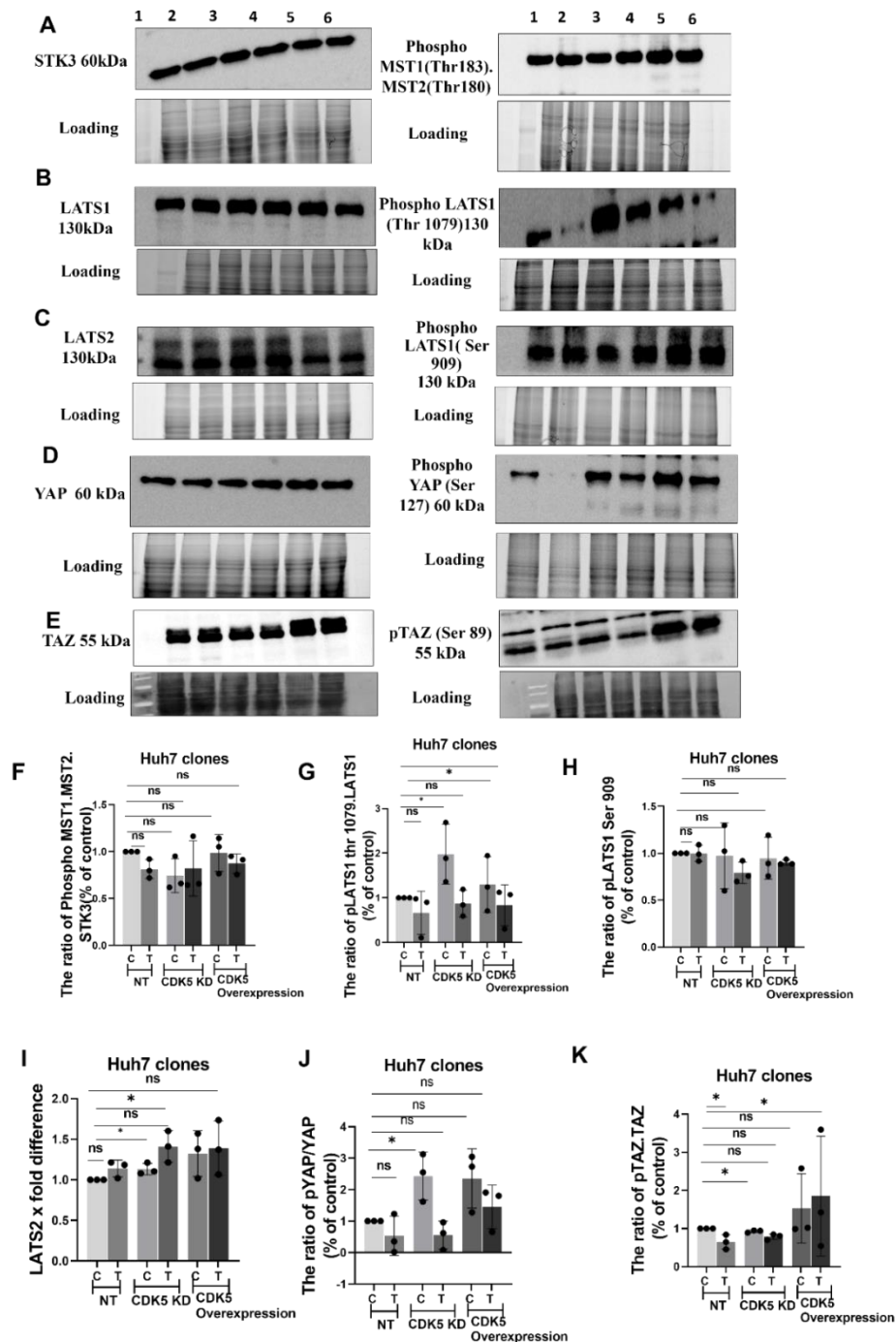
Figure 11 CDK5 influences the phosphorylation levels of kinases involved in Hippo pathway kinases.(A-E) Western blot analysis of the three cell groups (Huh7 nt, Huh7 CDK5 KD and Huh7 CDK5 overexpressing cells) for determination of protein expression of total and phosphorylates protein of upstream hippo kinases (A)MST2 & pMST1(Thr 180).pMST (Thr 183), (B) LATS1 & LATS1 (Thr 1079), (C) LATS2 & LATS1 (Ser 909) and downstream factors (D) YAP & pYAP (Ser 127) (E) TAZ & pTAZ (Ser 89) with (T) and without (C) thrombin treatment (0.5U, 15 min upstream and 1h downstream factors), Left panel describes the total protein and right panel phosphorylated protein(F-K) Determination of phospho levels to total levels of protein normalised to the loading control band intensity (Huh7 nt control cells). The experiments are performed in triplicates and bar graphs indicate mean ± SEM, 2way ANOVA test followed by Dunnett's multiple comparison test.

4.4 The kinase activity of CDK5 does not influence phospho YAP levels but the localisation of YAP in the nucleus.

We next investigated whether the kinase activity of CDK5 is responsible for regulating the levels of expression of phosphorylated kinases especially pLATS1(Thr 1079) and Pyap (Ser 127). For this, we inhibited the kinase activity of CDK5 with roscovitine. Huh7 nt control cells were treated with 50 µM roscovitine for 3h followed by thrombin treatment for 1h and then YAP and pYAP expression levels were determined. Later pYAP /total YAP ratio was calculated by normalising the values to control. (Figure 12A, B)

Interestingly, there was no significant change in the levels of phosphorylated YAP in roscovitine-treated cells compared to control cells (Figure 12B). The ratio of pYAP/total YAP did not vary in all groups but decreased with thrombin treatment as expected. (Figure 12B).

Next, we did immunostaining experiments to look for YAP localisation with roscovitine treatment and then calculated nucleus-to-cytoplasm intensity using the intensity ratio tool from Image J (Figure 12C, D). For this, cells were treated with 30 µM roscovitine for 30 min and then later with thrombin for 30 min. Compared to the control thrombin-treated group, the nucleus-to-cytoplasm intensity decreased in roscovitine thrombin- cotreated cells. Roscovitine seems to reduce nuclear YAP localisation after stimulation. With thrombin treatment alone, YAP got translocated in the nucleus and there was an increase in the percentage accumulation of activated YAP in the nucleus as expected. (Figure 12C, D).
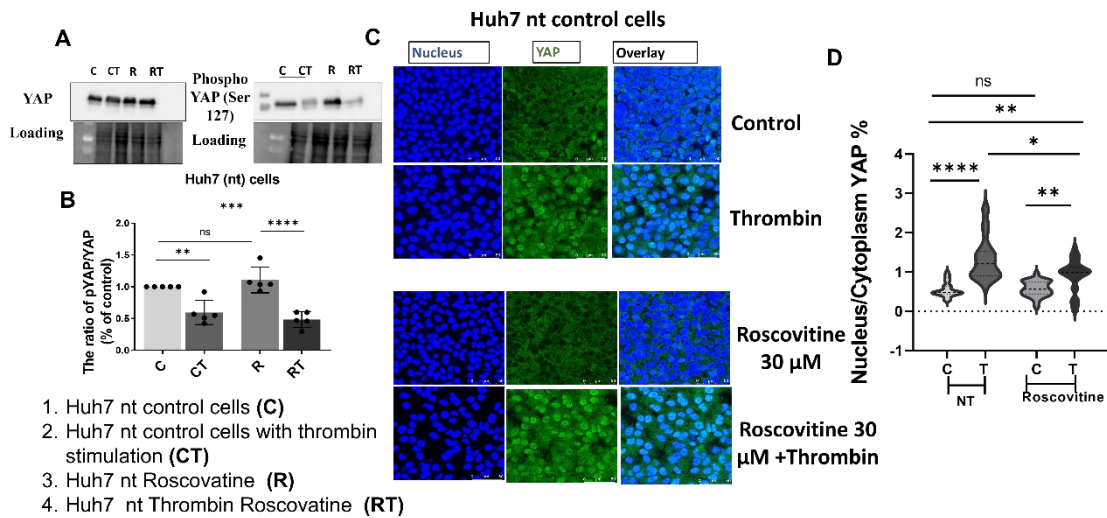
Figure 12 Kinase activity of CDK5 does not influence phospho YAP levels but localisation of YAP in the nucleus. To determine the effect of pharmacological inhibition of CDK5, cells were treated with Roscovitine, (A) Western Blot for YAP and pYAP on (Huh7 nt Control cells (C), Huh7 nt control cells with thrombin treatment (CT), Huh7 nt cells with roscovitine treatment (R), Huh7 nt cells treated with roscovitine followed by thrombin stimulation(RT) after roscovitine treatment. The cells were treated with roscovitine for (50 µM, 3h) followed by thrombin treatment for 0.5U, 1h. (B) Determination of phospho levels total YAP intensity in all the 4 groups (Huh7 nt control cells (C), Huh7 nt control cells with thrombin treatment (CT), Huh7 nt cells with roscovitine treatment (R), Huh7 nt cells treated with roscovitine followed by thrombin stimulation). All the values were normalised with Huh7 nt controls band intensity. The experiments are performed in triplicates and bar graph indicate mean ± SEM (One-Way ANOVA followed by Turkey's multiple comparison test). (C)Immunostaining for YAP in all the 4 groups, for these experiment cells were treated with roscovitine for (30 µM, 3h) followed by a thrombin stimulation (0.5U, 30 min), (D)Calculation of Nucleus to cytoplasm intensity ratio for YAP (The experiment was conducted in triplicates and for every repetition 10 images were taken into account, values are presented as mean ± SEM, unpaired t test followed by welches correction.

4.5 Compensation of loss of YAP activity by enhanced MRTF activity.

Next, we looked for the expression of YAP target genes CTGF and CYR 61 in the three cell groups (Figure 13A). There was no change in the expression of CTGF in nt control cells, CDK5 KD clones and Huh7 CDK5 overexpressing cells. However, surprisingly the expression of CYR 61 was more in CDK5 KD cells, almost double compared to the nt control cells. This was interesting because the YAP activity is lower with CDK5 KD, then how come the expression of CYR61, which is a YAP target gene increased? This gave rise to another question of cells finding a way to compensate for the loss of YAP activity by upregulating another mechanically sensitive pathway, such as the MRTF/SRF pathway sharing the common genes of interest. However, in CDK5 overexpressing cells the expression of CTGF and CYR 61 did not vary compared to Huh7 nt control cells. The

expression of CTGF and CYR61 increased with thrombin treatment in all three groups' cells as expected.

CYR61 is also a target gene of the MRTF pathway (Figure 13A). To determine the involvement of the MRTF/SRF pathway in compensating the loss of YAP activity, we conducted an MRTF reporter gene assay. The Luciferase/Renilla intensity ratio was determined as a readout of MRTF activity in both cell types (Figure 13B). Interestingly Huh7 CDK5 KD clones exhibited higher MRTF activity almost 2-fold compared to Huh7 nt control cells. It seemed that cells do find a way to recover for the loss of YAP activity from CDK5 knockdown by compensating it by upregulating the MRTF/SRF pathway. There was no significant further change observed with thrombin treatment.
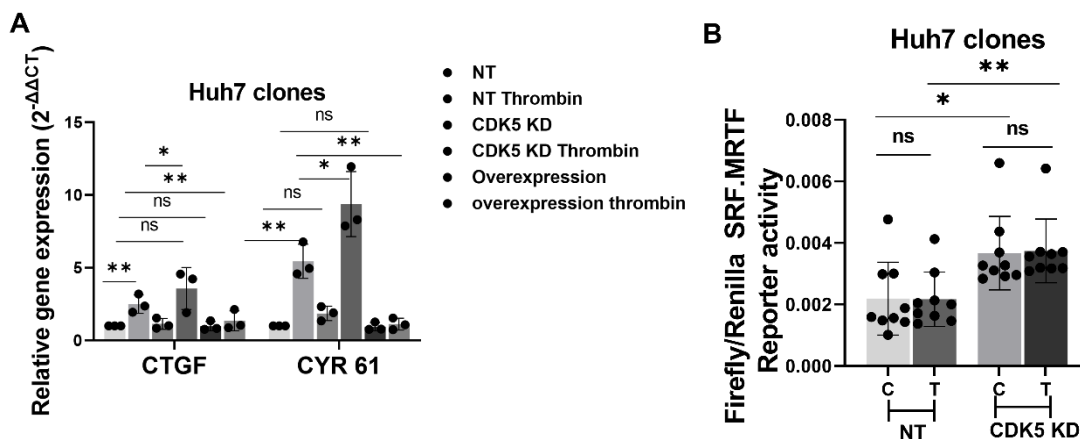
Figure 13 Compensation of loss of YAP activity by enhanced MRTF activity.(A) Quantitative PCR analysis of the YAP target genes CTGF and CYR 61 in all the 3 cell groups ,Huh7 nt control cells (NT), Huh7 CDK5 Knocdown cells (CDK5 KD) and Huh7 CDK5 overexpressing cells with and without thrombin treatment (all the experiments are done in triplicates ,values are presented as mean $\pm$ SEM , 2way ANOVA followed by Sidak's multiple comparison text. (B) Dual luciferase assay for SRF response element, comparing the MRTF SRK reporter activity in Huh7 nt control cells (NT) and Huh7 CDK5 knockdown cells (CDK5 KD) with (C) and without thrombin treatment (T) (the experiments were performed in triplicates and the values were presented as mean $\pm$ SEM, unpaired t test followed by welches correction).

4.6   Phosphoproteomics- connecting the dots

Protein mass spectrometry was conducted by Dr. Jan Stöckl (from the group of Dr. Fröhlich, Gene Center Munich, Laboratory of Functional Genome Analysis, LMU Munich). 5 biological samples for Huh7 nt and Huh7 CDK5 KD cells were

evaluated. A total of about 3300 proteins were identified in the whole proteome analysis. For the generation of phosphopeptide data matrix, similar workflow was applied. Only the peptides with phosphosite localisation possibilities of > 0.75 and score difference of > 5 were kept resulting in identification of about 5,000 phosphosites. After Welch´s t test was applied, a data matrix of about 1,600 total significantly differentially abundant proteins and 123 phosphosites were obtained.

Figure 14(A) represents the total proteins and phosphosites that are significantly differentially abundant in the two groups. Protein changes between Huh7 nt and Huh5 CDK5 KD cells were analysed with principal component analysis (PCA) hierarchical clustering (HCA). Unsupervised PCA showed that principal component 1 about 52.9% total explained variance highlighting a strong difference after CDK5 knockdown. It demonstrated that all the CDK5 KD replicates were identical while in case of NT there seemed to be some variation.There were overall significant changes in the proteins being upregulated and downregulated by CDK5 as demonstrated by volcano plots (Figure 14C) which displays negative Log_{10}p values and the $\log_2$ fold changes between Huh7 CDK5 KD cells and Huh7 NT cells. Next it was important to filter out the data in context to YAP and Hippo Signalling. So, we compared the top 400 significant upregulated and downregulated targets from our data set to the YAP interacting partners in a protein -protein interaction data base (BioGRID).

We made a list of about top 55 significant upregulated and downregulated genes with respect to the log 2-fold change in LFQ intensity as represented by a heat map and hierarchical clustering (Figure 15A). The Volcano plot in (Figure 15B) represents the overall changes in the significantly phosphorylated proteins. There was a number of established YAP, STK3 and CDK5 interacting partners that were significantly abundantly phosphorylated as displayed in Supplementary Table 17-19. To search for the missing link between STK3, YAP signalling and CDK5, we next filtered this list for the significant STK3 partners, and CDK5 substrates. We selected DLG5 as one of the potential targets which could be involved in the process. Disk large homolog 5 is a membrane associated guanylate kinase (MAGUK) protein which functions in cell polarity and regulates cellular proliferation

and differentiation[76]. There have been studies showing that it regulates Hippo pathway by acting as scaffold and linking MST1/2 with MARK3 (Par-1 polarity microtubule affinity regulating kinases 1/2/3 (MARK1/2/3) as well as promoting the hyperphosphorylation of MST1/2. It also inhibits the association of MST1/2 and LATS1/2 .Another study demonstrated that loss of DLG5 inhibited the Hippo pathway by decreasing the phosphorylation of MST1/2, LATS1/2 and MOB1 and increases YAP nuclear localisation[77] So, we decided to search if there is any relationship between CDK5 and DLG5. To test this hypothesis, we conducted co-immunoprecipitation experiments. Firstly, we pulled down CDK5 and detected DLG5 in the precipitate, and vice versa. It was interesting to see that when CDK5 was pulled down, we found a DLG5 band at 200 kDa. Accordingly, DLG5 seems to interact with CDK5 (Figure 15G, H). Also, the other way around when DLG5 was pulled down we found CDK5 at 35 kDa.CDK5, DLG5 and STK3 seem to form a scaffold protein and interact with each other. Further, we observed that DLG5 was phosphorylated in the cells both with and without stimulation with thrombin (Supplementary Figure 19). CDK5 belongs to the category of proline directed serine/threonine kinase group. The canonical sequence of amino acids recognised by CDK5 is Ser or Thr followed by a Pro. Therefore, the substrates recognised by CDK5 have (Ser/Thr)-Pro-X-(Arg/Lys/His) motif or a simple version of this motif, (Ser/Thr)-Pro. It is known to phosphorylate proteins possessing these canonical consensus sequence of amino acids [78] [79] . Phosphorylated sequence of DLG5 detected from our results also suggests that DLG5 is phosphorylated at (Ser/Thr)-Pro motif further insinuating to the possibility that DLG5 is phosphorylated by CDK5 (Supplementary Figure 19). YAP1 pull down experiments also show RAF-1, a major factor of the MAPK pathway, as one of the interacting partners of YAP1. (Supplementary Figure 22).
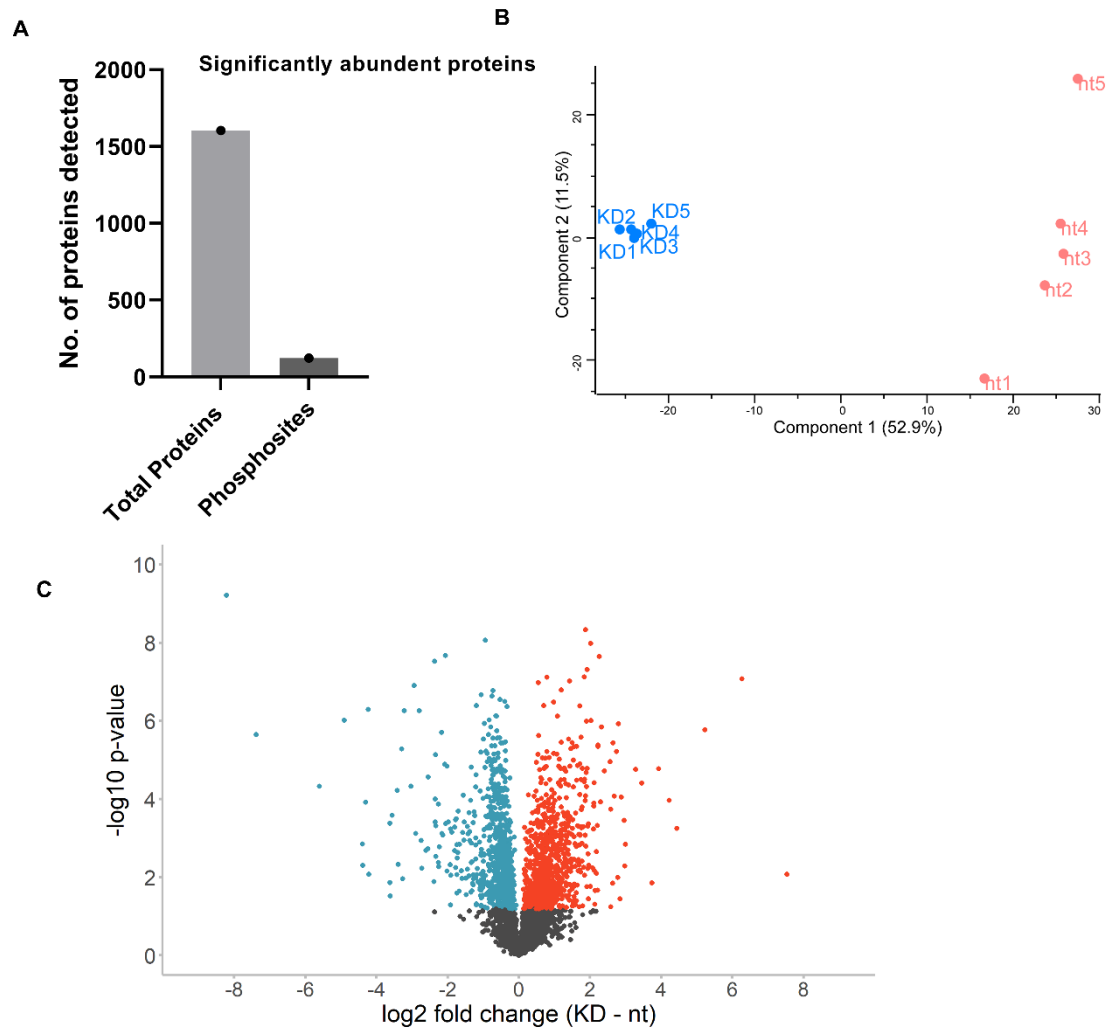
Figure 14 Whole proteome analysis representing. (A) Total number of significantly abundant total proteins and phosphosides identified. (B) Principal component analysis of protein abundance in Huh7 nt and Huh7 CDK5 KD ells. The PCA includes quantified proteins. Dots represent 5 biological replicates with blue Huh7 CDK5 KD and red Huh7 nt. (C) Volcano plot of phosphoproteomic data depicting the fold change of each phosphosite and the q value was calculated by performing a Welcht's t-test and a permutation test. Red circles show phosphosites which have significant increases. Blue circles how phosphosites which have significant decreases. Grey circles indicate no significant changes at all.

A
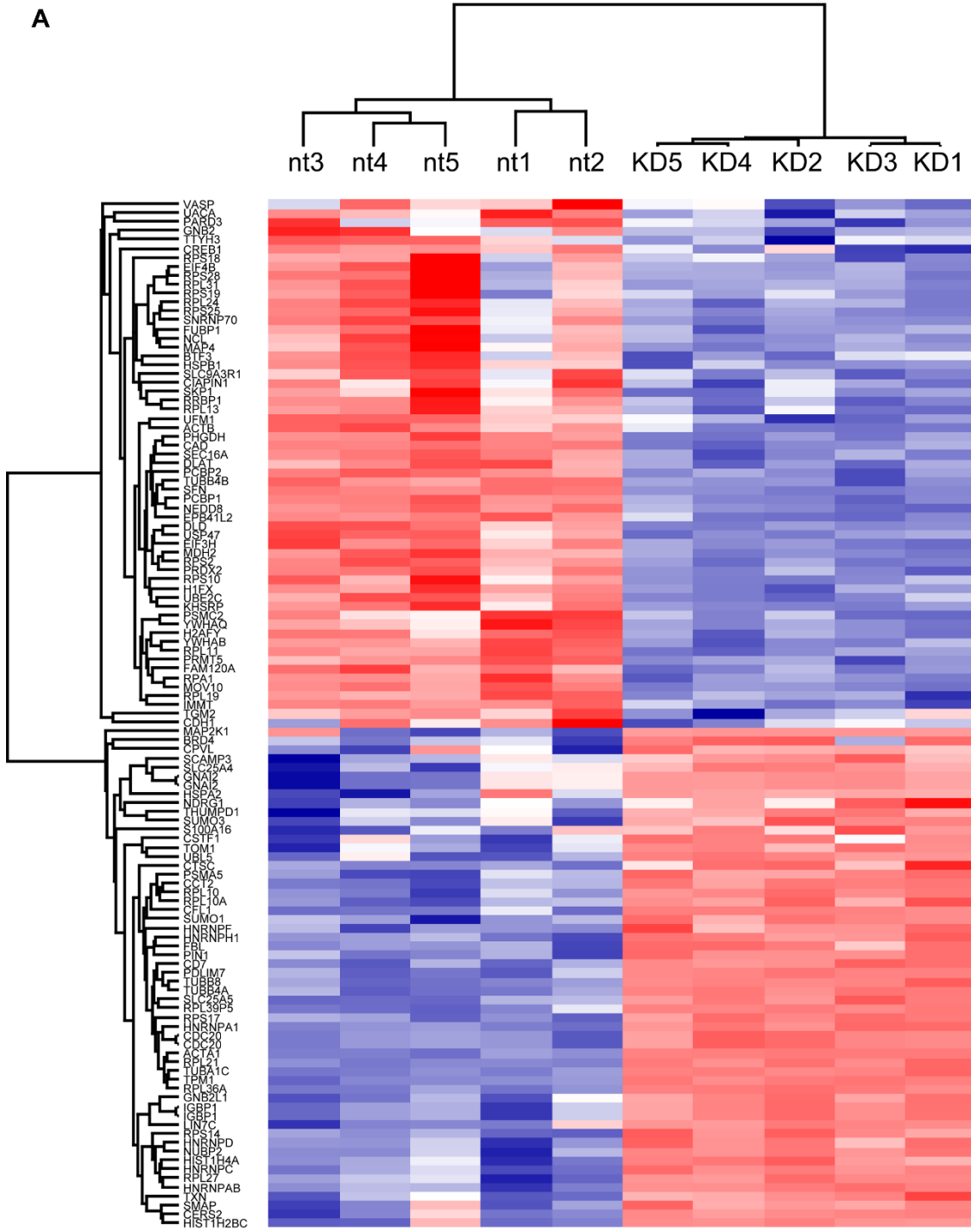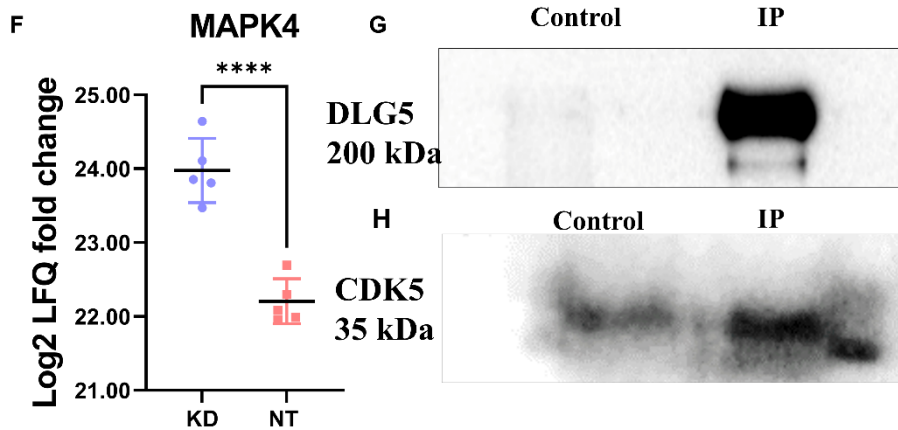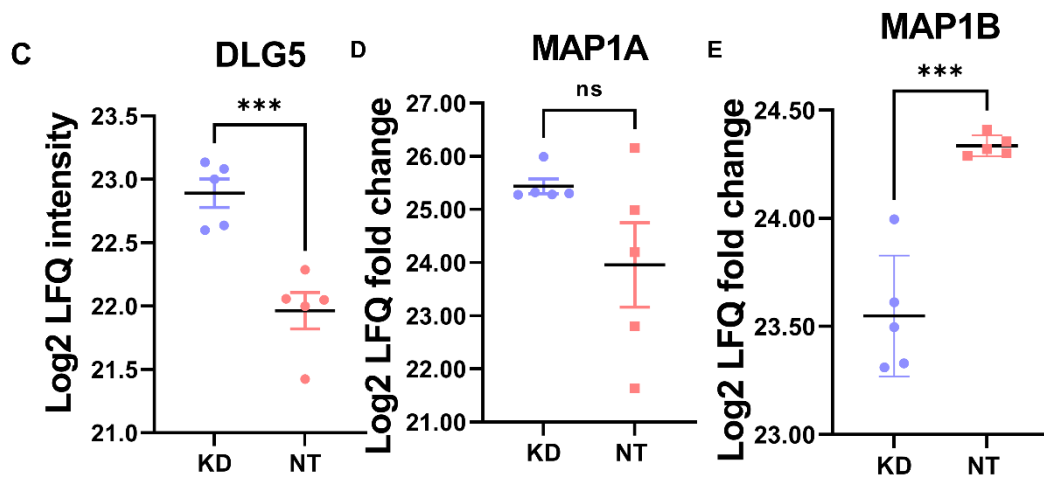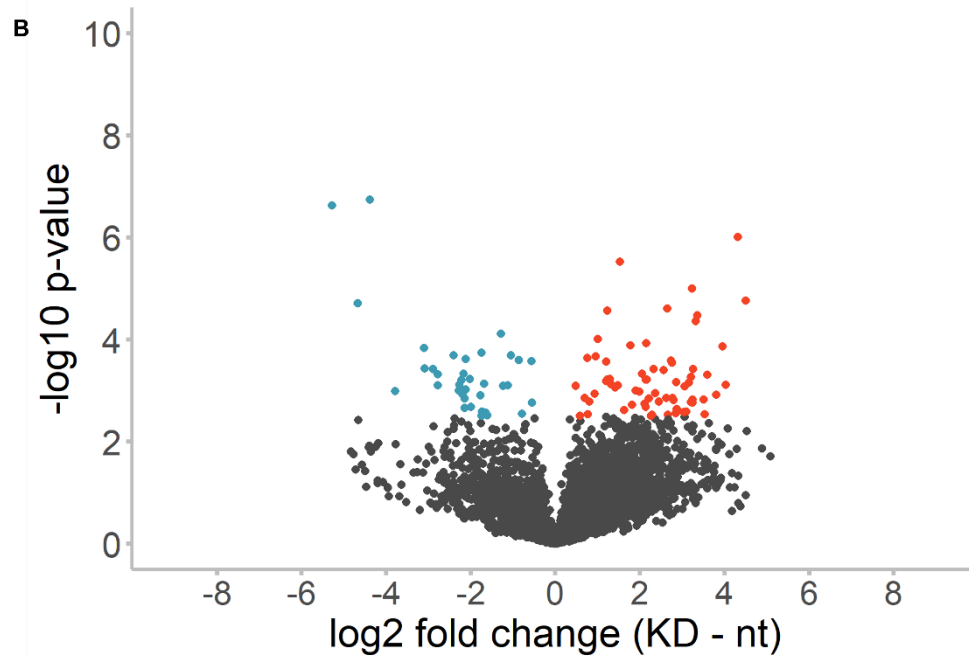
Figure 15 Significant phosphoproteome changes. (A) Heat map representing the significant changes in YAP interacting partners with respect to their Log 2 fold change in LFQ intensity, LFQ represents Label free quantified values from Mass spectroscopy analysis in the 5 replicates.(B) Volcano plot determining the changes in the phosphorylation statuses of the proteins in Huh7 CDK5 KD and Huh7 nt and Huh7 CDK5 KD cells with red dots representing upregulated proteins, blue dots representing downregulated and grey no change at all.(C-F) Differences in the phosphorylation intensities of Important interacting partners of CDK5 and STK3 represented in terms of Log2 LFQ change, LFQ represents label free quantified values from Mass spectroscopy analysis.(G-H) Co-immunoprecipitation experiments confirming this interaction (G) CDK5 antibody was utilised for IP and blotted for DLG5 (200 kDa), (H) DLG5 antibody was utilised for IP and blotted for CDK5 (35 kDa), experiments were done in triplicates to confirm this interaction. With control representing the bead control lane while IP representing the subsequent immunoprecipitation lane.

4.7   CDK5 influences cell behaviour in 3D

Since YAP signalling depends on matrix stiffness, we investigated the influence of CDK5 on YAP signalling in 3D spheroids embedded in a collagen gel. Spheroids from Huh7 CDK5 KD cells seem grow less than Huh7 nt spheroids (Figure 16A, B). Over the observation period, the cells migrated out of the spheroids (sprouting). Throughout 24h and 72h (Figure 16C, D) the migration of cells from Huh7 CDK5 KD spheroids was higher than Huh7 nt spheroids. Next, the cells were stained for YAP and the localisation of YAP was observed (Figure 16E, F). In both cases, YAP seems to be localised in the cytoplasm of spheroids because the cells were in tight contact. However, at the edges more active YAP was observed in the spheroids from both cell types. YAP exhibited the nucleus to cytoplasm shutting as on the edge's cells seem to be more active. The nucleus to cytoplasm intensity ratio of YAP was calculated by acquiring zoomed images at the edges. Plot profile line and plot profile area analysis of overall YAP intensity was done by calculating the mean grey value using Fiji image J. We observed that more YAP was on the edges of spheroids. However, the overall YAP localization seems to be the same in both cases with no significant differences. (Figure 16G-I
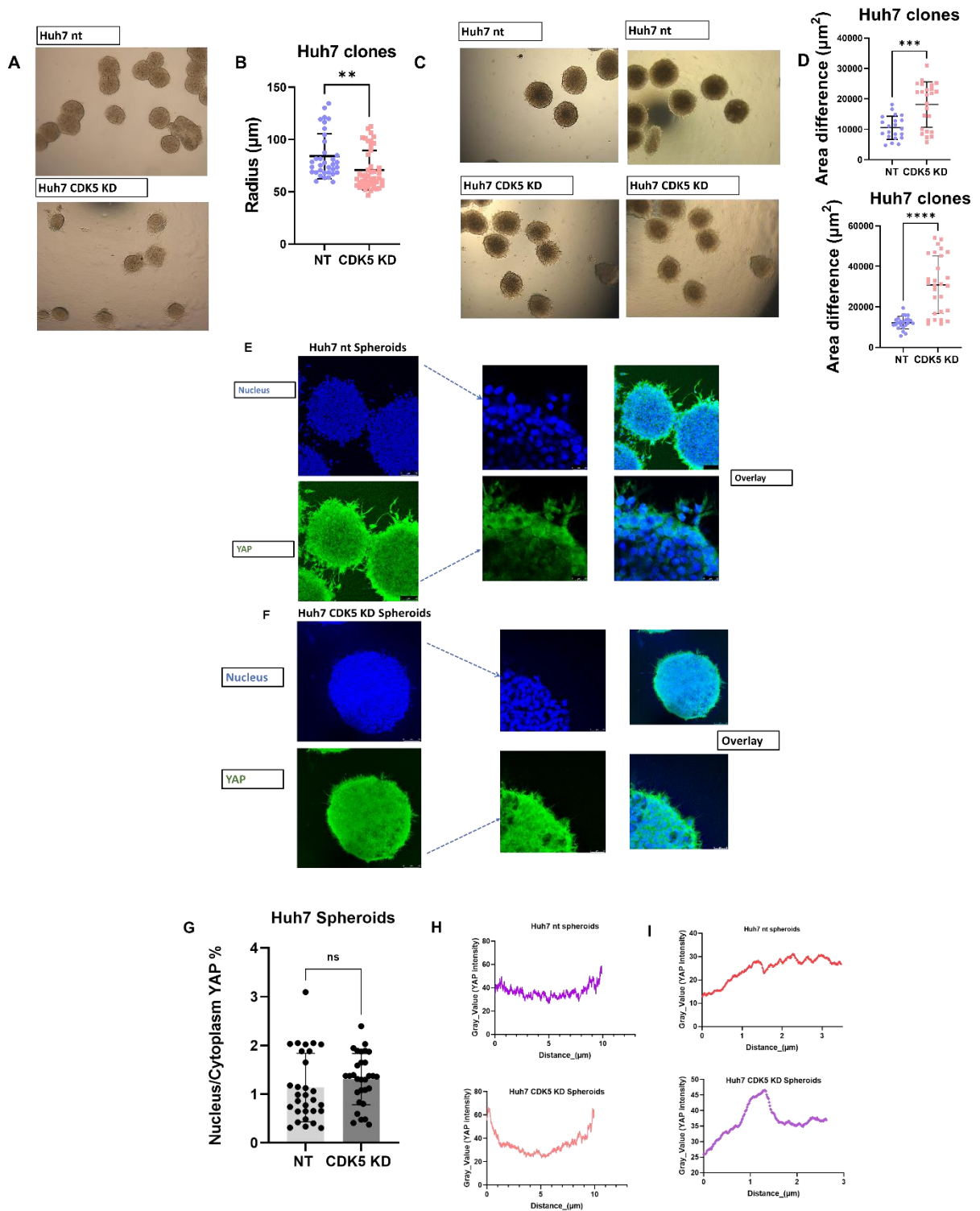
Figure 16 CDK5 influences cell behaviour in 3D. (A) Spheroids from Huh7 nt and Huh7 CDK5 KD cells prepared by hanging drop method and later embedded on collagen matrix (1.5 mg/ml) and imaged under bright field microscope (4x magnification, (B) Determination of radius of spheroids, radius was calculated with Fiji image J software, experiments were done in triplicates and overall a total of 30-35 spheroids were evaluated per repetition , radius is presented in terms of mean ± SEM , unpaired t test followed by welches correction.(C &D) Determination of migration/sprouting of Huh7 nt and Huh7 CDK5 KD cells from spheroids over a period of 24h and 72h, migration was calculated using Fiji image j tool by circling around the inner and outer circle around the circumference of spheroids, Experiments were done in triplicates and overall a total of 30-35 spheroids were evaluated , radius is presented in terms of mean ± SEM , unpaired t test followed by welches correction.(E &F) Immunostaining of YAP (green) for Huh7 nt and Huh7 CDK5 KD Spheroids along with their zoomed cross sections. The images were acquired in 20X objective.(G) Calculation of nucleus to cytoplasm % YAP intensity ratio for spheroids by evaluating the zoomed cross-section images acquired at 20X. Experiments were done in triplicates, with 5 spheroids for each cell type / repetition was evaluated, data is presented as mean ± SEM , unpaired t test followed by welches correction.(H&I) Evaluation of overall YAP intensity in Huh7 nt and Huh7 CDK5 KD spheroids by determination of mean grey values by plot profile line analysis and plot profile area analysis tool of image J software. Experiments were done in triplicates, with 5 spheroids for each cell type evaluated per repetition. Later the mean values of total 15 spheroids for all the repetitions were plotted in one single graph.

DISCUSSION

5 Discussion

5.1 Hippo pathway modulation by CDK5 and MST2 (STK3) interaction- an interdependent and unique mechanism

The Hippo signalling pathway plays an important role in the regulation of tissue growth, stem cell activity, and tissue architecture. It acts as the main signalling hub for the integration of various mechanisms such as cell-cell contact, cell density, cell shape, mechanotransduction, cell polarity and tissue architecture to regulate cell growth[80]. Mainly driven by the transcriptional activity of core kinases MST1/2 and LATS1/2, the Hippo pathway regulates the activity of oncoproteins YAP/TAZ through a series of phosphorylation events because of various regulatory feedback mechanisms occurring within the tissues. Hippo pathway dysregulation results in uncontrolled cell proliferation and tissue growth because of increased activity of YAP/TAZ[46 81] . Apart from its role in the central nervous system (CNS), CDK5 has been implicated in various types of cancers such as breast, prostate, HCC, breast, lung, ovarian and thyroid. However, its role in cancer is not well explored. It participates in various signalling pathways such as Notch, Rho GTPase and MAPK which lead to metastasis and regulates actin cytoskeleton and focal adhesions [56]. CDK5 also acts as a crucial regulator of angiogenesis by contributing to endothelial cell survival and regulating the expression of various angiogenic molecules such as VEGF and as hypoxia-inducible factor 1/ (HIF1/) target gene [82].

We herein identified a novel interaction between MST2 (STK3) and CDK5. MST1/2 acts as an upstream regulator of the Hippo pathway and regulates the expression of oncoprotein YAP and TAZ by phosphorylating LATS1/LATS2. LATS1/LATS2 are independently phosphorylated also by MAP4K kinases[83, 84] We demonstrate that following the interaction with MST2, CDK5 modulates the Hippo pathway and contributes to the activity of oncoproteins YAP/TAZ by tempering the levels of phosphorylated YAP. CDK5 attenuates the levels of phosphorylated upstream kinases LATS1 (Thr 1079) which in turn results in the regulation of YAP/TAZ activity. A recent study suggested that CDK5 attenuates the Hippo pathway impairing lung cancer progression and radio resistance via regulation of the overall expression levels of TAZ [85]. However, on the contrary, our results suggest that

CDK5 tempers with the phosphorylated levels of upstream kinase LATS1 and oncoprotein YAP. Going along the line, we successfully established that CDK5 participates in this entire process somewhere upstream by interacting with MST2 however not phosphorylating it.

5.2 The surprising activity of CDK5- not just a kinase but also a scaffolding protein

CDK5 is a kinase and has a wide variety of substrates which it phosphorylates through various mechanisms [86]. Apart from CNS development, all these substrates play an essential role in the regulation of cytoskeletal dynamics, pro and anti-migratory processes, synaptic functions and membrane cycling [56, 87]. However, our results suggest that pharmacological inhibition of kinase activity of CDK5 by Roscovitine [88]has no prominent effect on the phosphorylated YAP expression levels. This could mean that it is not essentially the kinase activity of CDK5 which is responsible for the modulation of the Hippo cascade and that it could act as a scaffolding protein. It is plausible that CDK5 provides a platform for the signalling molecules to assemble, promoting the localisation of signalling molecules at specific sites and coordinating positive and negative feedback signals for hippo pathway regulation. However, more studies are still required to elucidate this hypothesis.

5.3 Cells establishing their balance from the loss of YAP activity

Further previous studies have highlighted that MRTF-SRF and YAP-TEAD pathways mutually depend on and functionally interact even though they do not share a common DNA targeting factor[89]. CTGF and CYR 61 are the most prevalent YAP target genes in the Hippo pathway and are involved in tumour formation, fibrosis, and wound healing and tend to be the shared targets for the MRTF-SRF pathway as well [90] They contain the binding sites for both SRF and TEAD. It has been previously reported that activation of either pathway potentiates the activity of the other indirectly and both depend on cytoskeletal dynamics. Our findings go along the line and suggest that in Huh7 cells, loss of CDK5 has no prominent effect, especially on the expression of CYR 61 but even leads to its enhanced expression.

This is contrary to the loss of active YAP. It seems that cells find a way to recover and compensate for the loss of YAP activity by upregulating MRTF-SRF activity as suggested by reporter gene assay results.

5.4 Phosphoproteomics – giving deep insights and clearing out the picture

CDK5 is a major kinase, and, consequently, its knockdown influences the entire proteome and phosphoproteome Interestingly, there were also major alterations in the levels of YAP interacting partners, and significant changes in the phospho levels of important YAP, STK3 and CDK5 interacting partners (supplementary table 17-19). Further, STK3 is also a kinase and has several documented binding partners such as SARAH domain containing proteins SAV1 and RASSF proteins[91]. DLG5 is one such interacting partner of STK3 belonging to this category of interactors [12]. It has been well established in literature that DLG5 directly regulates the Hippo pathway by promoting hyperphosphorylation of STK3 through recruitment of microtubule affinity regulating kinase 3 (MARK3) to STK3. DLG5 also assists in interaction of STK3 and LATS1 [76, 77]. Phosphoproteomics also suggested that there was a major change in the phosphorylation status of DLG5 after CDK5 knockdown.

Further going along the line Hippo pathway is known to interact and cross talk with several other pathways such as, MRTF, MAPK pathway, JNK signalling, (GPCR) signalling pathways, Wnt signalling etc [92]. Looking into the common similarities of these pathways with the Hippo pathway and finding the common connections and links of STK3 and CDK5, we also found MAPK signalling to be of interest in this context. RAF-1 is a major activator of the MAPK pathway and has been known to interact with STK3 and to influence the expression of YAP/TAZ.[84] The interaction of RAF-1 with STK3 leads to the activation of the RAF/MEK1/ERK (MAPK) signalling cascade[84]. CDK5 is well known to phosphorylate MEK1 and downregulate RAF/MEK1/ERK (MAPK) pathways[93]. CDK5 interacts with STK3, therefore, a link between Hippo pathway and MAPK signalling via CDK5 dependent mechanism cannot be ruled out. Moreover, DLG5 is also known to

enhance RAS/RAF/MEK1/ERK (MAPK) signalling cascade by varying the phosphorylation levels of Extracellular signal-regulated kinase (ERK) 1/2.[77]

Also, our findings have proved that CDK5 not only interacts with STK3 but also with DLG5. CDK5 could also phosphorylate DLG5 as DGL5 share a common phosphorylation motif with CDK5.Therefore, the plausibility of further CDK5 acting as scaffold bringing MAPK and Hippo signalling cascade together cannot be ruled out. It might serve as a scaffold by bringing DLG5 and STK3 together and facilitating the interaction between DLG5 and STK3. CDK5 also seems to assist in modulating the phosphorylation of way upstream kinases. Phosphorylation of DLG5 is upregulated in Huh7 CDK5 KD cells, as revealed by phosphoproteomics results. DLG5 directly regulates Hippo pathway, therefore after CDK5 knockdown we have hyperactivation of Hippo pathway and therefore lower activity of YAP/TAZ, which is a result of interaction of CDK5 with DLG5 and CDK5 with STK3 (Figure 17). CDK5 is a versatile kinase, and it is interesting to find how it regulates the phosphorylation statuses of various kinases and signalling cascades altogether by providing a platform and also modulating cross talks between different pathways.

5.5 3D microenvironment and CDK5

CDK5 is also known to be involved in angiogenesis in endothelial cells. It has been reported in the literature that it regulates lamellipodia formation and contributes to endothelial cell migration by remodelling the actin cytoskeleton [94]. It also regulates the expression of VEGF and hypoxia-inducible factor-1α (HIF-1α) in endothelial cells.[95]. It has been reported previously that spheroids from Huh7 nt cultured together with Huvecs promoted the proliferation and gene expression of HCC-related genes by activating cytokine signalling and mimicking gene expression in liver cancer. HUVECs also induced angiogenesis and vessel formation in Huh7 nt spheroids by activating EMT transition and angiogenic pathways[94]. On the contrary, it has also been reported that in corneal epithelial cells, p39-CDK5 formation stabilizes the stress fibres formation and inhibits migration of epithelial cells by augmenting the Rho-ROCK signalling dependent phosphorylation of Myosin. [96]. It also directly phosphorylates the scaffold protein muskelin and further

facilitates the phosphorylation of myosin by Rho-ROCK signalling further stabilizing the stress fibres. Inhibition of CDK5 decreases the phosphorylation of the myosin regulatory light chain (MRLC) resulting in disruption of stress fibre organisation and increased epithelial cell migration [97].

Our results indicate that Huh7 CDK5 KD spheroids have more sprouting over time compared to spheroids from Huh7 nt which could suggest a possibility of a negative feedback loop being facilitated by CDK5 because of various physiological changes in the cellular 3D environment over time. However, there was no distinguishable difference in the activation of YAP and its distribution in both the spheroids cultured on collagen gels. These studies implicate that CDK5 has some consequences on overall cell behaviour in 3D, but more studies are required to reflect on this.

In the end, to summarise our results provide new insights into how CDK5-MST2 interaction results in the transcriptional regulation of the hippo pathway in Huh7 cells, which could be a new therapeutic strategy for the development of CDK5 inhibitors which target the hippo pathway. However, there is more to exploring the versatile nature of CDK5. Further studies are required to completely decipher the behaviour of CDK5 in regulating various mechanical signalling pathways.
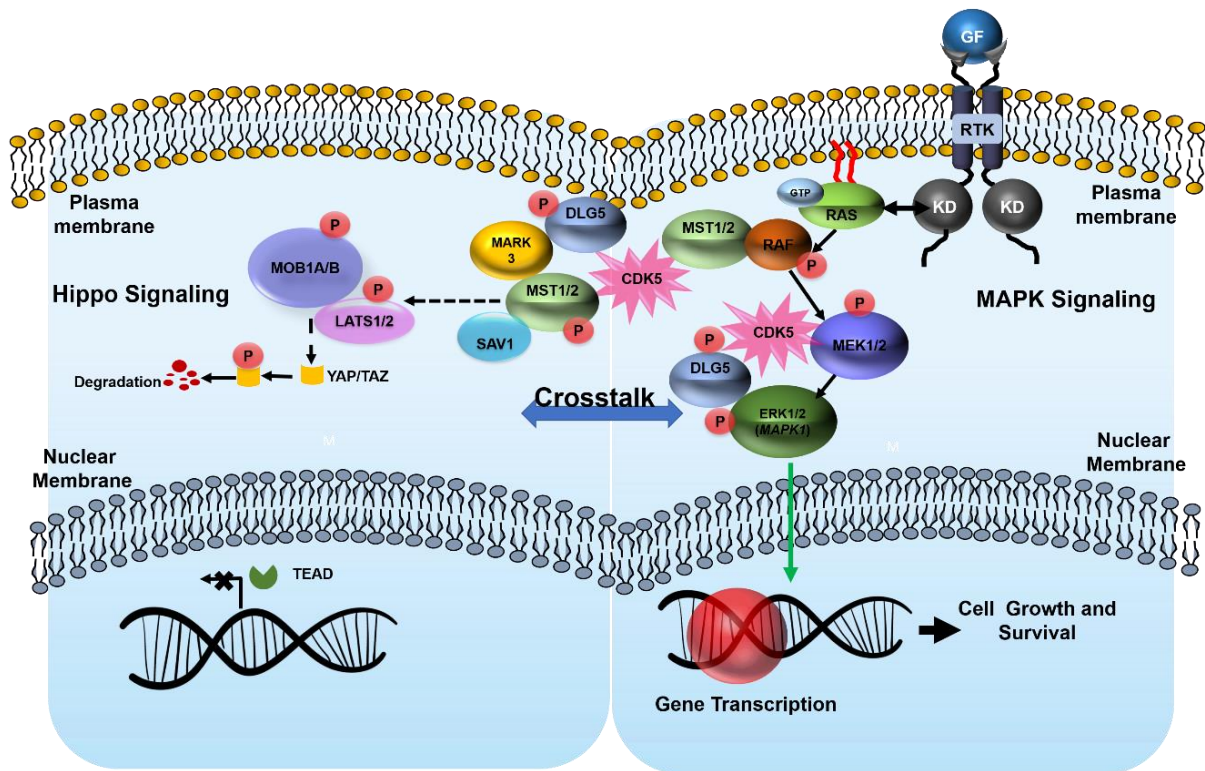
Figure 17 Proposed mechanism of CDK5 mediated cross talk of Hippo pathway with MAPK pathway. In general MAPK pathway functions by translocation of ERK into the nucleus which leads to gene transcription and cell proliferation. It has been well described before in literature that MST kinases interact with MAPK factor RAF, CDK5 interacts with MEK and DLG5 further interacts with ERK kinases. There seem to be some sort of CDK5 mediated cross talk between Hippo ad MAPK pathways where CDK5 acts as a scaffold and bring the signalling kinases together from both the pathways.

REFERENCES

6 References

(1) Dey, A.; Varelas, X.; Guan, K.-L. Targeting the Hippo pathway in cancer, fibrosis, wound healing and regenerative medicine. *Nature reviews Drug discovery* **2020**, *19* (7), 480-494.

(2) Bae, S. J.; Luo, X. Activation mechanisms of the Hippo kinase signaling cascade. *Bioscience reports* **2018**, *38* (4).

(3) Boopathy, G. T.; Hong, W. Role of hippo pathway-YAP/TAZ signaling in angiogenesis. *Frontiers in cell and developmental biology* **2019**, *7*, 49.

(4) Galan, J. A.; Avruch, J. MST1/MST2 protein kinases: regulation and physiologic roles. *Biochemistry* **2016**, *55* (39), 5507-5519.

(5) Hansen, C. G.; Moroishi, T.; Guan, K.-L. YAP and TAZ: a nexus for Hippo signaling and beyond. *Trends in cell biology* **2015**, *25* (9), 499-513.

(6) Hong, W.; Guan, K.-L. The YAP and TAZ transcription co-activators: key downstream effectors of the mammalian Hippo pathway. In *Seminars in cell & developmental biology*, 2012; Elsevier: Vol. 23, pp 785-793.

(7) Hillmer, R. E.; Link, B. A. The roles of Hippo signaling transducers Yap and Taz in chromatin remodeling. *Cells* **2019**, *8* (5), 502.

(8) Haskins, J. W.; Nguyen, D. X.; Stern, D. F. Neuregulin 1–activated ERBB4 interacts with YAP to induce Hippo pathway target genes and promote cell migration. *Science signaling* **2014**, *7* (355), ra116-ra116.

(9) Nishio, M.; Sugimachi, K.; Goto, H.; Wang, J.; Morikawa, T.; Miyachi, Y.; Takano, Y.; Hikasa, H.; Itoh, T.; Suzuki, S. O. Dysregulated YAP1/TAZ and TGF-β signaling mediate hepatocarcinogenesis in Mob1a/1b-deficient mice. *Proceedings of the National Academy of Sciences* **2016**, *113* (1), E71-E80.

(10) Callus, B. A.; Verhagen, A. M.; Vaux, D. L. Association of mammalian sterile twenty kinases, Mst1 and Mst2, with hSalvador via C-terminal coiled-coil domains, leads to its stabilization and phosphorylation. *The FEBS journal* **2006**, *273* (18), 4264-4276.

(11) Thompson, B. J.; Sahai, E. MST kinases in development and disease. *Journal of Cell Biology* **2015**, *210* (6), 871-882. Qin, F.; Tian, J.; Zhou, D.; Chen, L. Mst1 and Mst2 kinases: regulations and diseases. *Cell & bioscience* **2013**, *3*, 1-9.

(12) Sanchez-Sanz, G.; Matallanas, D.; Nguyen, L. K.; Kholodenko, B. N.; Rosta, E.; Kolch, W.; Buchete, N.-V. MST2-RASSF protein–protein interactions through SARAH domains. *Briefings in Bioinformatics* **2016**, *17* (4), 593-602.

(13) Bae, S. J.; Ni, L.; Osinski, A.; Tomchick, D. R.; Brautigam, C. A.; Luo, X. SAV1 promotes Hippo kinase activation through antagonizing the PP2A phosphatase STRIPAK. *Elife* **2017**, *6*, e30278.

(14) Terrell, E. M.; Morrison, D. K. Ras-mediated activation of the Raf family kinases. *Cold Spring Harbor perspectives in medicine* **2019**, *9* (1), a033746.

(15) O'Neill, E.; Rushworth, L.; Baccarini, M.; Kolch, W. Role of the kinase MST2 in suppression of apoptosis by the proto-oncogene product Raf-1. *Science* **2004**, *306* (5705), 2267-2270.

(16) Chen, Y.-A.; Lu, C.-Y.; Cheng, T.-Y.; Pan, S.-H.; Chen, H.-F.; Chang, N.-S. WW domain-containing proteins YAP and TAZ in the hippo pathway as key regulators in stemness maintenance, tissue homeostasis, and tumorigenesis. *Frontiers in Oncology* **2019**, *9*, 60.

(17) Holden, J. K.; Cunningham, C. N. Targeting the hippo pathway and cancer through the TEAD family of transcription factors. *Cancers* **2018**, *10* (3), 81.

(18) Piccolo, S.; Dupont, S.; Cordenonsi, M. The biology of YAP/TAZ: hippo signaling and beyond. *Physiological reviews* **2014**.

(19) Feigin, M. E.; Muthuswamy, S. K. Polarity proteins regulate mammalian cell–cell junctions and cancer pathogenesis. *Current opinion in cell biology* **2009**, *21* (5), 694-700.

(20) Chan, S. W.; Lim, C. J.; Chong, Y. F.; Pobbati, A. V.; Huang, C.; Hong, W. Hippo pathway-independent restriction of TAZ and YAP by angiomotin. *Journal of Biological Chemistry* **2011**, *286* (9), 7018-7026.

(21) Silvis, M. R.; Kreger, B. T.; Lien, W.-H.; Klezovitch, O.; Rudakova, G. M.; Camargo, F. D.; Lantz, D. M.; Seykora, J. T.; Vasioukhin, V. α-catenin is a tumor suppressor that controls cell accumulation by regulating the localization and activity of the transcriptional coactivator Yap1. *Science signaling* **2011**, *4* (174), ra33-ra33.

(22) Schlegelmilch, K.; Mohseni, M.; Kirak, O.; Pruszak, J.; Rodriguez, J. R.; Zhou, D.; Kreger, B. T.; Vasioukhin, V.; Avruch, J.; Brummelkamp, T. R. Yap1 acts downstream of α-catenin to control epidermal proliferation. *Cell* **2011**, *144* (5), 782-795.

(23) Zanconato, F.; Cordenonsi, M.; Piccolo, S. YAP and TAZ: a signalling hub of the tumour microenvironment. *Nature Reviews Cancer* **2019**, *19* (8), 454-464.

(24) Mackay, D. J.; Hall, A. Rho GTPases. *Journal of Biological Chemistry* **1998**, *273* (33), 20685-20688.

(25) Yu, F.-X.; Zhao, B.; Panupinthu, N.; Jewell, J. L.; Lian, I.; Wang, L. H.; Zhao, J.; Yuan, H.; Tumaneng, K.; Li, H. Regulation of the Hippo-YAP pathway by G-protein-coupled receptor signaling. *Cell* **2012**, *150* (4), 780-791.

(26) Yasuda, D.; Kobayashi, D.; Akahoshi, N.; Ohto-Nakanishi, T.; Yoshioka, K.; Takuwa, Y.; Mizuno, S.; Takahashi, S.; Ishii, S. Lysophosphatidic acid–induced YAP/TAZ activation promotes developmental angiogenesis by repressing Notch ligand Dll4. *The Journal of clinical investigation* **2019**, *129* (10), 4332-4349. Tocci, P.; Blandino, G.; Bagnato, A. YAP and endothelin-1 signaling: an emerging alliance in cancer. *Journal of Experimental & Clinical Cancer Research* **2021**, *40* (1), 1-12.

(27) Hoy, J. J.; Parra, N. S.; Park, J.; Kuhn, S.; Iglesias-Bartolome, R. Protein kinase A inhibitor proteins (PKIs) divert GPCR-Gαs-cAMP signaling towards EPAC and ERK activation and are involved in tumor growth. *FASEB journal: official publication of the Federation of American Societies for Experimental Biology* **2020**, *34* (10), 13900.

(28) Seo, J.; Kim, J. Regulation of Hippo signaling by actin remodeling. *BMB reports* **2018**, *51* (3), 151.

(29) Azzolin, L.; Panciera, T.; Soligo, S.; Enzo, E.; Bicciato, S.; Dupont, S.; Bresolin, S.; Frasson, C.; Basso, G.; Guzzardo, V. YAP/TAZ incorporation in the β-catenin destruction complex orchestrates the Wnt response. *Cell* **2014**, *158* (1), 157-170.

(30) Moroishi, T.; Park, H. W.; Qin, B.; Chen, Q.; Meng, Z.; Plouffe, S. W.; Taniguchi, K.; Yu, F.-X.; Karin, M.; Pan, D. A YAP/TAZ-induced feedback

mechanism regulates Hippo pathway homeostasis. *Genes & development* **2015**, *29* (12), 1271-1284.

(31) Zhang, W.; Liu, H. T. MAPK signal pathways in the regulation of cell proliferation in mammalian cells. *Cell Research* **2002**, *12*, 9-18.

(32) Lin, K. C.; Moroishi, T.; Meng, Z.; Jeong, H.-S.; Plouffe, S. W.; Sekido, Y.; Han, J.; Park, H. W.; Guan, K.-L. Regulation of Hippo pathway transcription factor TEAD by p38 MAPK-induced cytoplasmic translocation. *Nature cell biology* **2017**, *19* (8), 996-1002.

(33) Basson, M. A. Signaling in cell differentiation and morphogenesis. *Cold Spring Harbor perspectives in biology* **2012**, *4* (6), a008151.

(34) Calses, P. C.; Crawford, J. J.; Lill, J. R.; Dey, A. Hippo pathway in cancer: aberrant regulation and therapeutic opportunities. *Trends in cancer* **2019**, *5* (5), 297-307.

(35) Li, F.-L.; Guan, K.-L. The two sides of Hippo pathway in cancer. In *Seminars in Cancer Biology*, 2022; Elsevier: Vol. 85, pp 33-42.

(36) Moon, S.; Yeon Park, S.; Woo Park, H. Regulation of the Hippo pathway in cancer biology. *Cellular and Molecular Life Sciences* **2018**, *75*, 2303-2319.

(37) Ouyang, L.; Shi, Z.; Zhao, S.; Wang, F. T.; Zhou, T. T.; Liu, B.; Bao, J. K. Programmed cell death pathways in cancer: a review of apoptosis, autophagy and programmed necrosis. *Cell proliferation* **2012**, *45* (6), 487-498.

(38) Lin, L.; Sabnis, A. J.; Chan, E.; Olivas, V.; Cade, L.; Pazarentzos, E.; Asthana, S.; Neel, D.; Yan, J. J.; Lu, X. The Hippo effector YAP promotes resistance to RAF- and MEK-targeted cancer therapies. *Nature genetics* **2015**, *47* (3), 250-256.

(39) Zeng, R.; Dong, J. The Hippo signaling pathway in drug resistance in cancer. *Cancers* **2021**, *13* (2), 318.

(40) Loh, C.-Y.; Chai, J. Y.; Tang, T. F.; Wong, W. F.; Sethi, G.; Shanmugam, M. K.; Chong, P. P.; Looi, C. Y. The E-cadherin and N-cadherin switch in epithelial-to-mesenchymal transition: signaling, therapeutic implications, and challenges. *Cells* **2019**, *8* (10), 1118.

(41) Wang, Z.; Sun, L.; Liang, S.; Liu, Z.-c.; Zhao, Z.-y.; Yang, J.; Wang, D.; Yang, D.-Q. GPER stabilizes F-actin cytoskeleton and activates TAZ via PLCβ-PKC and Rho/ROCK-LIMK-Cofilin pathway. *Biochemical and biophysical research communications* **2019**, *516* (3), 976-982.

(42) Taniguchi, K.; Wu, L.-W.; Grivennikov, S. I.; De Jong, P. R.; Lian, I.; Yu, F.-X.; Wang, K.; Ho, S. B.; Boland, B. S.; Chang, J. T. A gp130–Src–YAP module links inflammation to epithelial regeneration. *Nature* **2015**, *519* (7541), 57-62.

(43) Yang, W.; Yang, S.; Zhang, F.; Cheng, F.; Wang, X.; Rao, J. Influence of the Hippo-YAP signalling pathway on tumor associated macrophages (TAMs) and its implications on cancer immunosuppressive microenvironment. *Annals of Translational Medicine* **2020**, *8* (6).

(44) Tian, Z.; Hou, X.; Liu, W.; Han, Z.; Wei, L. Macrophages and hepatocellular carcinoma. *Cell & bioscience* **2019**, *9*, 1-10.

(45) Lai, C.; Wang, K.; Zhao, Z.; Zhang, L.; Gu, H.; Yang, P.; Wang, X. CC motif chemokine ligand 2 (CCL2) mediates acute lung injury induced by lethal influenza H7N9 virus. *Frontiers in microbiology* **2017**, *8*, 587.

(46) Harvey, K. F.; Zhang, X.; Thomas, D. M. The Hippo pathway and human cancer. *Nature Reviews Cancer* **2013**, *13* (4), 246-257.

(47) Wang, J.; Liu, S.; Heallen, T.; Martin, J. F. The Hippo pathway in the heart: pivotal roles in development, disease, and regeneration. *Nature Reviews Cardiology* **2018**, *15* (11), 672-684.

(48) Wang, S.; Zhou, L.; Ling, L.; Meng, X.; Chu, F.; Zhang, S.; Zhou, F. The crosstalk between hippo-YAP pathway and innate immunity. *Frontiers in immunology* **2020**, *11*, 323.

(49) Taha, Z.; J. Janse van Rensburg, H.; Yang, X. The Hippo pathway: immunity and cancer. *Cancers* **2018**, *10* (4), 94.

(50) Panciera, T.; Azzolin, L.; Cordenonsi, M.; Piccolo, S. Mechanobiology of YAP and TAZ in physiology and disease. *Nature reviews Molecular cell biology* **2017**, *18* (12), 758-770.

(51) Cai, X.; Wang, K.-C.; Meng, Z. Mechanoregulation of YAP and TAZ in cellular homeostasis and disease progression. *Frontiers in cell and developmental biology* **2021**, *9*, 673599.

(52) Dasgupta, I.; McCollum, D. Control of cellular responses to mechanical cues through YAP/TAZ regulation. *Journal of Biological Chemistry* **2019**, *294* (46), 17693-17706.

(53) Totaro, A.; Panciera, T.; Piccolo, S. YAP/TAZ upstream signals and downstream responses. *Nature cell biology* **2018**, *20* (8), 888-899.

(54) Helfman, D. M.; Pawlak, G. Myosin light chain kinase and acto-myosin contractility modulate activation of the ERK cascade downstream of oncogenic Ras. *Journal of cellular biochemistry* **2005**, *95* (5), 1069-1080.

(55) Zanconato, F.; Cordenonsi, M.; Piccolo, S. YAP/TAZ at the roots of cancer. *Cancer cell* **2016**, *29* (6), 783-803.

(56) Pozo, K.; Bibb, J. A. The emerging role of Cdk5 in cancer. *Trends in cancer* **2016**, *2* (10), 606-618.

(57) Pareek, T. K.; Lam, E.; Zheng, X.; Askew, D.; Kulkarni, A. B.; Chance, M. R.; Huang, A. Y.; Cooke, K. R.; Letterio, J. J. Cyclin-dependent kinase 5 activity is required for T cell activation and induction of experimental autoimmune encephalomyelitis. *Journal of Experimental Medicine* **2010**, *207* (11), 2507-2519.

(58) Shupp, A.; Casimiro, M. C.; Pestell, R. G. Biological functions of CDK5 and potential CDK5 targeted clinical treatments. *Oncotarget* **2017**, *8* (10), 17373.

(59) Maitra, S.; Vincent, B. Cdk5-p25 as a key element linking amyloid and tau pathologies in Alzheimer's disease: Mechanisms and possible therapeutic interventions. *Life Sciences* **2022**, 120986.

(60) Hisanaga, S.-i.; Saito, T. The regulation of cyclin-dependent kinase 5 activity through the metabolism of p35 or p39 Cdk5 activator. *Neurosignals* **2003**, *12* (4-5), 221-229.

(61) Sharma, S.; Zhang, T.; Michowski, W.; Rebecca, V. W.; Xiao, M.; Ferretti, R.; Suski, J. M.; Bronson, R. T.; Paulo, J. A.; Frederick, D. Targeting the cyclin-dependent kinase 5 in metastatic melanoma. *Proceedings of the National Academy of Sciences* **2020**, *117* (14), 8001-8012.

(62) Do, P. A.; Lee, C. H. The role of CDK5 in tumours and tumour microenvironments. *Cancers* **2020**, *13* (1), 101.

(63) Carter, A. M.; Kumar, N.; Herring, B.; Tan, C.; Guenter, R.; Telange, R.; Howse, W.; Viol, F.; McCaw, T. R.; Bickerton, H. H. Cdk5 drives formation of heterogeneous pancreatic neuroendocrine tumors. *Oncogenesis* **2021**, *10* (12), 83.

(64) Hsu, F.-N.; Chen, M.-C.; Chiang, M.-C.; Lin, E.; Lee, Y.-T.; Huang, P.-H.; Lee, G.-S.; Lin, H. Regulation of androgen receptor and prostate cancer growth by cyclin-dependent kinase 5. *Journal of Biological Chemistry* **2011**, *286* (38), 33141-33149.

(65) Liu, W.; Li, J.; Song, Y.-S.; Li, Y.; Jia, Y.-H.; Zhao, H.-D. Cdk5 links with DNA damage response and cancer. *Molecular cancer* **2017**, *16*, 1-9.

(66) Liang, Q.; Li, L.; Zhang, J.; Lei, Y.; Wang, L.; Liu, D.-X.; Feng, J.; Hou, P.; Yao, R.; Zhang, Y. CDK5 is essential for TGF-β1-induced epithelial-mesenchymal transition and breast cancer progression. *Scientific reports* **2013**, *3* (1), 1-13.

(67) Zheng, Y.-L.; Li, B.-S.; Kanungo, J.; Kesavapany, S.; Amin, N.; Grant, P.; Pant, H. C. Cdk5 Modulation of mitogen-activated protein kinase signaling regulates neuronal survival. *Molecular biology of the cell* **2007**, *18* (2), 404-413.

(68) Tian, B.; Yang, Q.; Mao, Z. Phosphorylation of ATM by Cdk5 mediates DNA damage signalling and regulates neuronal death. *Nature cell biology* **2009**, *11* (2), 211-218.

(69) Caron, J. M.; Han, X.; Contois, L.; Vary, C. P.; Brooks, P. C. The HU177 collagen epitope controls melanoma cell migration and experimental metastasis by a CDK5/YAP-dependent mechanism. *The American journal of pathology* **2018**, *188* (10), 2356-2368.

(70) Ardelt, M. A.; Fröhlich, T.; Martini, E.; Müller, M.; Kanitz, V.; Atzberger, C.; Cantonati, P.; Meßner, M.; Posselt, L.; Lehr, T. Inhibition of cyclin-dependent kinase 5: a strategy to improve sorafenib response in hepatocellular carcinoma therapy. *Hepatology* **2019**, *69* (1), 376-393.

(71) Mascia, T.; Santovito, E.; Gallitelli, D.; Cillo, F. Evaluation of reference genes for quantitative reverse-transcription polymerase chain reaction normalization in infected tomato plants. *Molecular plant pathology* **2010**, *11* (6), 805-816.

(72) Cox, J.; Mann, M. MaxQuant enables high peptide identification rates, individualized p.p.b.-range mass accuracies and proteome-wide protein quantification. *Nat Biotechnol* **2008**, *26* (12), 1367-1372. DOI: 10.1038/nbt.1511. Tyanova, S.; Temu, T.; Cox, J. The MaxQuant computational platform for mass spectrometry-based shotgun proteomics. *Nat Protoc* **2016**, *11* (12), 2301-2319. DOI: 10.1038/nprot.2016.136.

(73) Tyanova, S.; Temu, T.; Sinitcyn, P.; Carlson, A.; Hein, M. Y.; Geiger, T.; Mann, M.; Cox, J. The Perseus computational platform for comprehensive analysis of (prote)omics data. *Nat Methods* **2016**, *13* (9), 731-740. DOI: 10.1038/nmeth.3901.

(74) Team, R. C.; Team, R. C. R: A language and environment for statistical computing. R Foundation for Statistical Computing, Vienna, Austria, 4.0. 5. 2021.

(75) Mo, J.-S.; Yu, F.-X.; Gong, R.; Brown, J. H.; Guan, K.-L. Regulation of the Hippo–YAP pathway by protease-activated receptors (PARs). *Genes & development* **2012**, *26* (19), 2138-2143.

(76) Kwan, J.; Sczaniecka, A.; Arash, E. H.; Nguyen, L.; Chen, C.-C.; Ratkovic, S.; Klezovitch, O.; Attisano, L.; McNeill, H.; Emili, A. DLG5 connects cell polarity and Hippo signaling protein networks by linking PAR-1 with MST1/2. *Genes & development* **2016**, *30* (24), 2696-2709.

(77) Liu, J.; Li, J.; Li, P.; Wang, Y.; Liang, Z.; Jiang, Y.; Li, J.; Feng, C.; Wang, R.; Chen, H. Loss of DLG5 promotes breast cancer malignancy by inhibiting the Hippo signaling pathway. *Scientific reports* **2017**, *7* (1), 42125.

(78) Borquez, D. A.; Olmos, C.; Alvarez, S.; Di Genova, A.; Maass, A.; Gonzalez-Billault, C. Bioinformatic survey for new physiological substrates of Cyclin-dependent kinase 5. *Genomics* **2013**, *101* (4), 221-228.

(79) Contreras-Vallejos, E.; Utreras, E.; Bórquez, D. A.; Prochazkova, M.; Terse, A.; Jaffe, H.; Toledo, A.; Arruti, C.; Pant, H. C.; Kulkarni, A. B. Searching for novel Cdk5 substrates in brain by comparative phosphoproteomics of wild type and Cdk5−/− mice. *PloS one* **2014**, *9* (3), e90363.

(80) Mo, J. S.; Park, H. W.; Guan, K. L. The Hippo signaling pathway in stem cell biology and cancer. *EMBO reports* **2014**, *15* (6), 642-656.

(81) Zhao, B.; Wei, X.; Li, W.; Udan, R. S.; Yang, Q.; Kim, J.; Xie, J.; Ikenoue, T.; Yu, J.; Li, L. Inactivation of YAP oncoprotein by the Hippo pathway is involved in cell contact inhibition and tissue growth control. *Genes & development* **2007**, *21* (21), 2747-2761.

(82) Herzog, J.; Ehrlich, S. M.; Pfitzer, L.; Liebl, J.; Fröhlich, T.; Arnold, G. J.; Mikulits, W.; Haider, C.; Vollmar, A. M.; Zahler, S. Cyclin-dependent kinase 5 stabilizes hypoxia-inducible factor-1α: a novel approach for inhibiting angiogenesis in hepatocellular carcinoma. *Oncotarget* **2016**, *7* (19), 27108.

(83) Meng, Z.; Moroishi, T.; Mottier-Pavie, V.; Plouffe, S. W.; Hansen, C. G.; Hong, A. W.; Park, H. W.; Mo, J.-S.; Lu, W.; Lu, S. MAP4K family kinases act in parallel to MST1/2 to activate LATS1/2 in the Hippo pathway. *Nature communications* **2015**, *6* (1), 8357.

(84) Feng, R.; Gong, J.; Wu, L.; Wang, L.; Zhang, B.; Liang, G.; Zheng, H.; Xiao, H. MAPK and Hippo signaling pathways crosstalk via the RAF-1/MST-2 interaction in malignant melanoma. *Oncology reports* **2017**, *38* (2), 1199-1205.

(85) Zeng, Y.; Liu, Q.; Wang, Y.; Tian, C.; Yang, Q.; Zhao, Y.; Liu, L.; Wu, G.; Xu, S. CDK5 activates hippo signaling to confer resistance to radiation therapy via upregulating TAZ in lung cancer. *International Journal of Radiation Oncology* *Biology* Physics* **2020**, *108* (3), 758-769. Merk, H.; Zhang, S.; Lehr, T.; Müller, C.; Ulrich, M.; Bibb, J. A.; Adams, R. H.; Bracher, F.; Zahler, S.; Vollmar, A. M. Inhibition of endothelial Cdk5 reduces tumor growth by promoting non-productive angiogenesis. *Oncotarget* **2016**, *7* (5), 6088. Lopes, J. P.; Agostinho, P. Cdk5: multitasking between physiological and pathological conditions. *Progress in neurobiology* **2011**, *94* (1), 49-63.

(86) Pao, P.-C.; Tsai, L.-H. Three decades of Cdk5. *Journal of Biomedical Science* **2021**, *28* (1), 1-17.

(87) Dhavan, R.; Tsai, L.-H. A decade of CDK5. *Nature reviews Molecular cell biology* **2001**, *2* (10), 749-759.

(88) Tomov, N.; Surchev, L.; Wiedenmann, C.; Döbrössy, M.; Nikkhah, G. Roscovitine, an experimental CDK5 inhibitor, causes delayed suppression of microglial, but not astroglial recruitment around intracerebral dopaminergic grafts. *Experimental neurology* **2019**, *318*, 135-144.

(89) Liu, C.-Y.; Chan, S. W.; Guo, F.; Toloczko, A.; Cui, L.; Hong, W. MRTF/SRF dependent transcriptional regulation of TAZ in breast cancer cells. *Oncotarget* **2016**, *7* (12), 13706. Foster, C. T.; Gualdrini, F.; Treisman, R. Mutual dependence of the MRTF–SRF and YAP–TEAD pathways in cancer-associated fibroblasts is indirect and mediated by cytoskeletal dynamics. *Genes & development* **2017**, *31* (23-24), 2361-2375.

(90) Shome, D.; von Woedtke, T.; Riedel, K.; Masur, K. The HIPPO transducer YAP and its targets CTGF and Cyr61 drive a paracrine signalling in cold atmospheric plasma-mediated wound healing. *Oxidative Medicine and Cellular Longevity* **2020**, *2020*.

(91) Donninger, H.; Schmidt, M. L.; Mezzanotte, J.; Barnoud, T.; Clark, G. J. Ras signaling through RASSF proteins. In *Seminars in cell & developmental biology*, 2016; Elsevier: Vol. 58, pp 86-95.

(92) Kim, M.; Jho, E.-h. Cross-talk between Wnt/β-catenin and Hippo signaling pathways: a brief review. *BMB reports* **2014**, *47* (10), 540.

(93) Sharma, P.; Sharma, M.; Amin, N. D.; Sihag, R. K.; Grant, P.; Ahn, N.; Kulkarni, A. B.; Pant, H. C. Phosphorylation of MEK1 by cdk5/p35 down-regulates the mitogen-activated protein kinase pathway. *Journal of Biological Chemistry* **2002**, *277* (1), 528-534.

(94) Jung, H.-R.; Kang, H. M.; Ryu, J.-W.; Kim, D.-S.; Noh, K. H.; Kim, E.-S.; Lee, H.-J.; Chung, K.-S.; Cho, H.-S.; Kim, N.-S. Cell spheroids with enhanced aggressiveness to mimic human liver cancer in vitro and in vivo. *Scientific Reports* **2017**, *7* (1), 1-14.

(95) Shabalina, E. Y.; Skorova, E. Y.; Chudakova, D.; Anikin, V.; Reshetov, I.; Mynbaev, O.; Petersen, E. The matrix-dependent 3D spheroid model of the migration of non-small cell lung cancer: a step towards a rapid automated screening. *Frontiers in Molecular Biosciences* **2021**, *8*, 610407.

(96) Tripathi, B. K.; Zelenka, P. S. Cdk5-dependent regulation of Rho activity, cytoskeletal contraction, and epithelial cell migration via suppression of Src and p190RhoGAP. *Molecular and cellular biology* **2009**, *29* (24), 6488-6499.

(97) Tripathi, B. K.; Lowy, D. R.; Zelenka, P. S. The Cdk5 activator P39 specifically links muskelin to myosin II and regulates stress fiber formation and actin organization in lens. *Experimental cell research* **2015**, *330* (1), 186-198.

APPENDIX

7 Appendix

7.1 Supplementary information

7.1.1 Supplementary figures
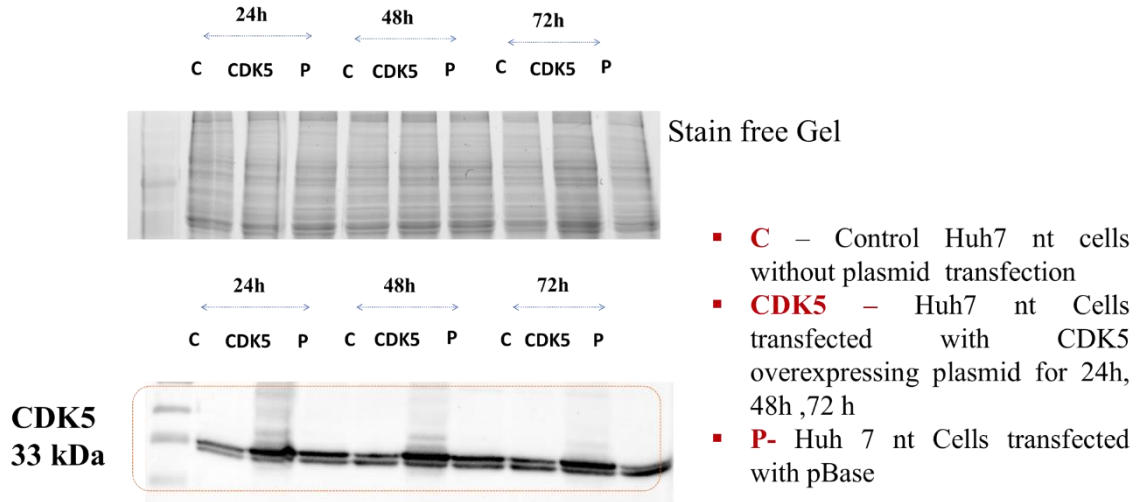
Figure 18 Huh7 nt control cells were transfected with CDK5 Overexpressing plasmid using lipofectamine 3000 and CDK5 expression was determined over a period of 24h, 48h and 72h.
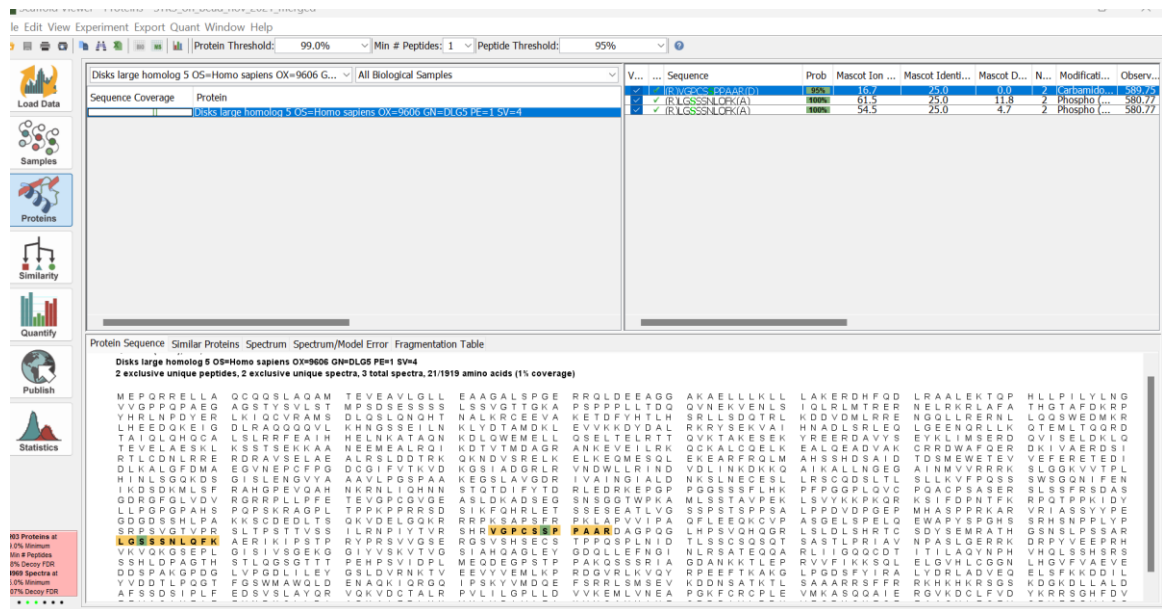
Figure 19 Sequence of DLG5 detected in phosphoproteomics with green representing the phosphorylated sites in phosphoproteomics of Huh7 nt cells with and without thrombin treatment.

84
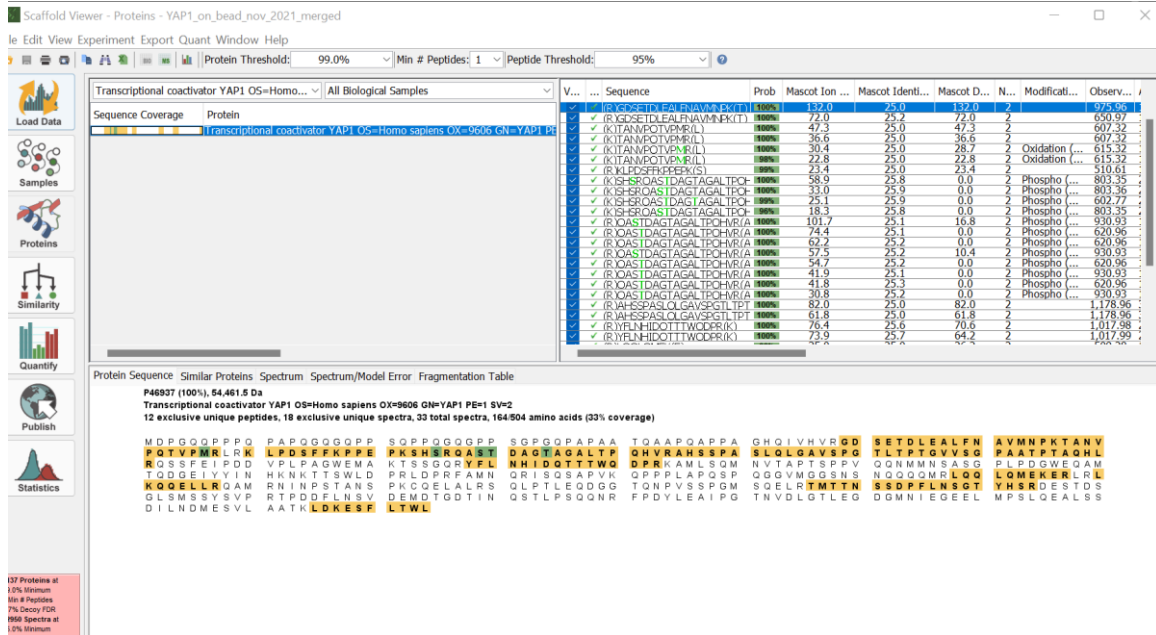
Figure 20 Sequence of YAP detected in phosphoproteomics with green representing the phosphorylated sites in YAP1 Co-IP experiments done on Huh7 nt cells.
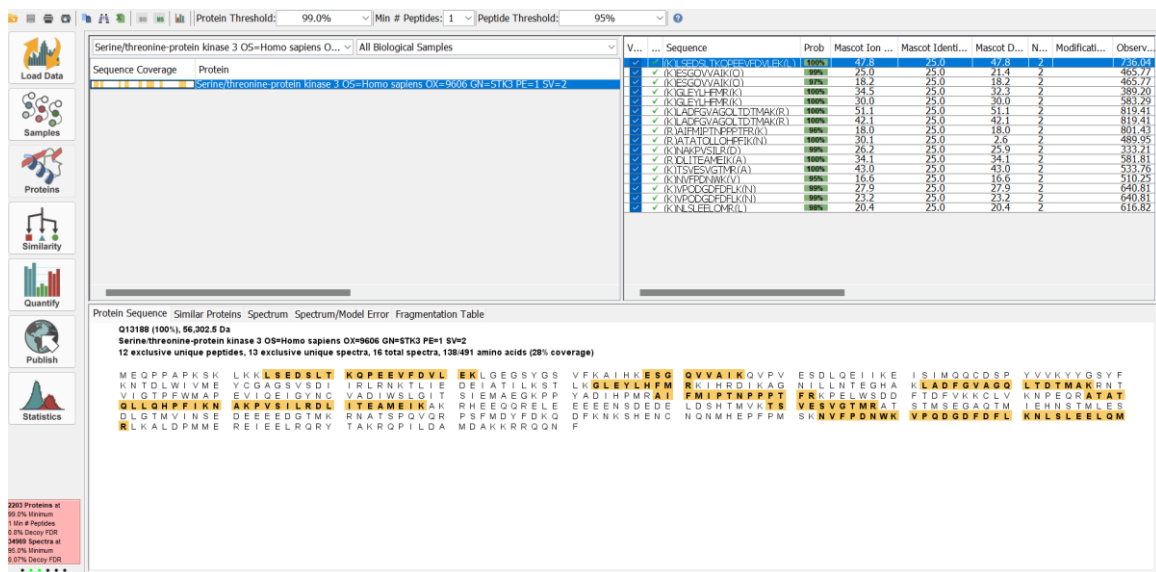
Figure 21 Sequence of STK3 detected in phosphoproteomics STK3 Co-IP experiments done on Huh7 nt cells.
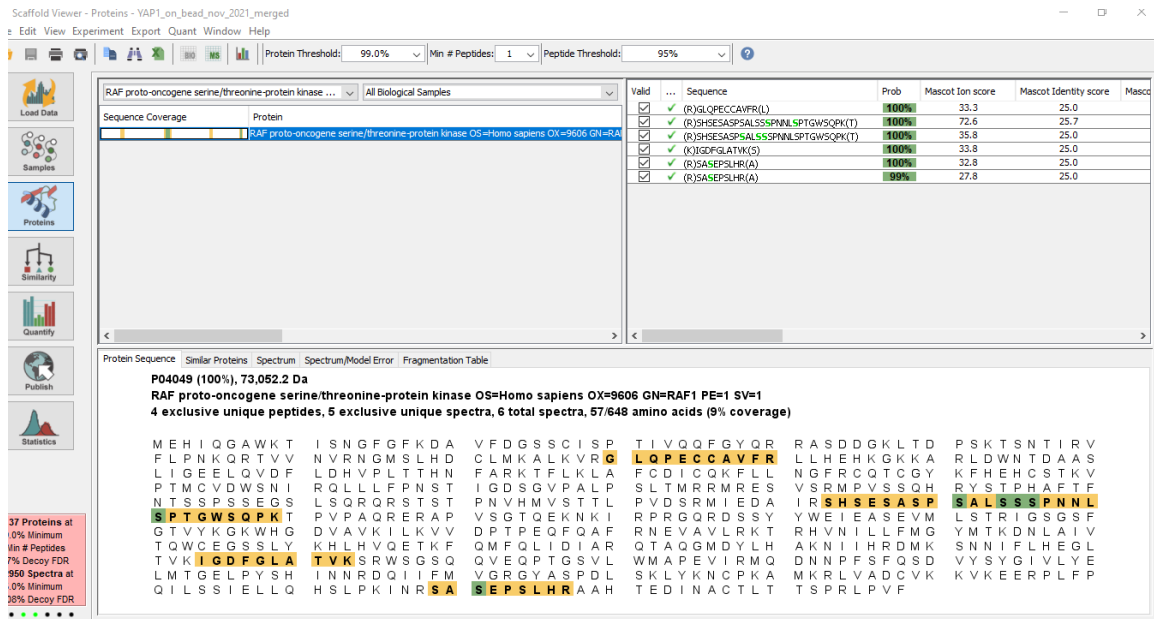
Figure 22 Sequence of RAF-1 detected in phosphoproteomics YAP1 Co-IP experiments done on Huh7 nt cells.
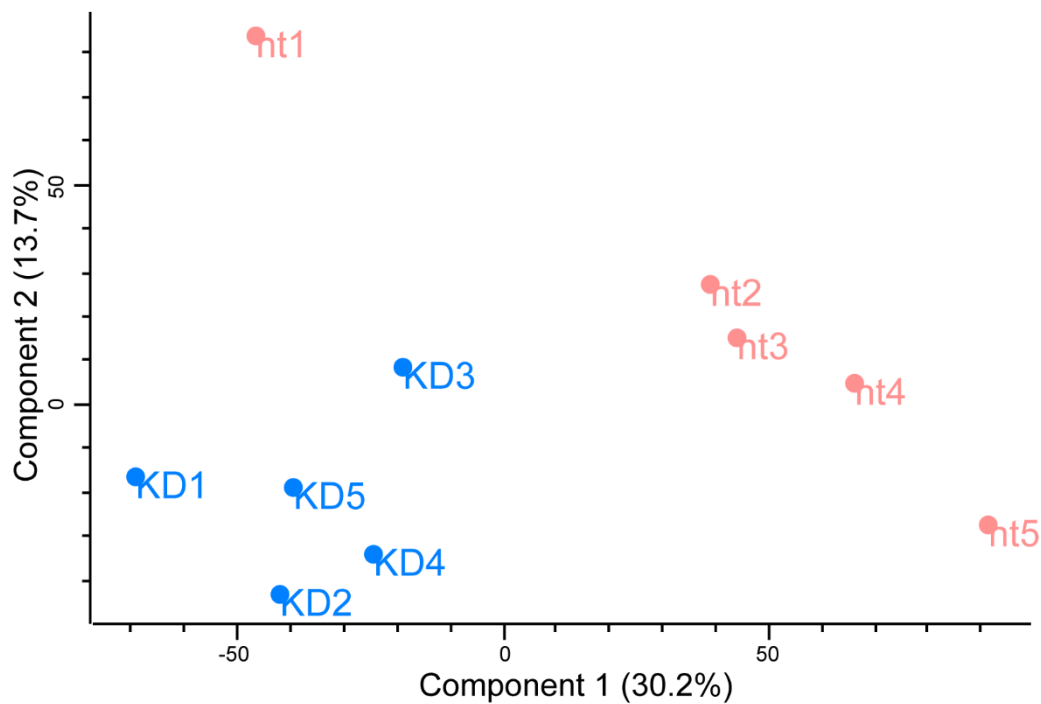
Figure 23 Principal component analysis of phosphoproteins in Huh7 nt and Huh7 CDK5 KD ells. The PCA includes quantified proteins. Dots represent 5 biological replicates with blue Huh7 CDK5 KD and red Huh7 nt.

7.1.2 Supplementary Tables

Sequencing results

Insert identity	frequency
Homo sapiens serine/threonine kinase 3 (STK3)	9
Homo sapiens ring finger protein 2 (RNF2)	25
Homo sapiens leucine rich repeat containing 6 (LRRC6)	1
Cyclin 1 (CCN1)	60
Phosphyglucomutase 1	1
Homo sapiens pyridoxal dependent decarboxylase domain containing 2, pseudogene (PDXDC2P) on chromosome16	21
Homo sapiens serine/threonine kinase 3 (STK3)	36

Table 16 Sequencing results yeast two hybrid system

Protein names	Gene names	significant	p-value	q-value	Log2 fold change
CDK5 Interacting partners					
ActivatedRNA polymerase II transcriptional coactivator p15	SUB1	+	0.002	0.040	0.81
Death-associated protein 1	DAP	+	0.000	0.052	1.53
Fatty acid synthase [Acyl-carrier-protein] S-acetyltransferase	FASN	+	0.001	0.040	-1.69

High mobility group protein HMG-I/HMG-Y	HMGA1	+	0.001	0.036	1.42
Nestin	NES	+	0.000	0.041	4.31
Microtubule-associated protein 1B; MAP1B heavy chain; MAP1 light chain LC1	MAP1B	+	0.003	0.050	-0.79
Microtubule-associated protein 1B; MAP1B heavy chain; MAP1 light chain LC1	MAP1B	+	0.003	0.050	-0.79

Table 17 Important significantly abundantly phosphorylated interactors of CDK5 upregulated and downregulated after CDK5 knockdown with Log2 fold change representing changes in LFQ intensity values.

YAP interacting partners					
Apoptotic chromatin condensation inducer in the nucleus	ACIN1	+	0.001	0.041	1.23
Fatty acid synthase; [Acyl-carrier-protein] S-acetyltransferase; [Acyl-carrier-protein] S-malonyltransferase	FASN	+	0.001	0.040	-1.69
Heterogeneous nuclear ribonucleoprotein A1; Heterogeneous nuclear ribonucleoprotein A1, N-terminally processed	HNRNPA1	+	0.000	0.075	-2.40

Microtubule-associated protein 4	MAP4	+	0.000	0.086	1.77
Nucleolin	NCL	+	0.000	0.092	2.15
Serine/arginine repetitive matrix protein 2	SRRM2	+	0.001	0.037	3.80
Tight junction protein ZO-2	TJP2	+	0.000	0.083	3.31
Ubiquitin-associated protein 2-like	UBAP2L	+	0.000	0.090	1.00
\Vimentin	VIM	+	0.002	0.043	2.14

Table 18 Important significantly abundantly phosphorylated interactors of YAP upregulated and downregulated after CDK5 knockdown with Log2 fold change representing changes in LFQ intensity values.

MST Interacting partners					
Disks large homolog 5	DLG5	+	0.001	0.037	0.93
Microtubule-associated protein 4	MAP4	+	0.000	0.086	1.77

Table 19 Important significantly abundantly phosphorylated interactors of STK3 upregulated and downregulated after CDK5 knockdown with Log2 fold change representing changes in LFQ intensity values.

7.2 Abbreviations

Abbreviation	Term
°C	Degree celcius
AJ	Adherens junctions
CCND1	Cyclin D1
CDK5	Cyclin dependent kinase 5
DLG5	Disk large homolog 5
DMEM	Dulbecco's Modified Eagle Medium
DMSO	Dimethyl sulfoxide
DNA	Deoxyribonucleic acid
DTT	1,4-dithiothreitol
ECL	Enhanced chemiluminescence
ECM	Extracellular matrix
EDTA	Ethylenediaminetetraacetic acid
EGFR	Endothelial growth factor receptor
ERK	Extracellular signal regulated protein kinase
FCS	Fetal calf serum
FOXM1	Forkhead box protein M1
GFP	Green fluorescent protein
H	Hour
HCC	Hepatocellular carcinoma
HIF-1α	Hypoxia-inducible factor 1 alpha
KD	Knockdown
LATS	Large tumor suppressor
MAP4K	Mitogen activated protein kinase 4
MAPK	Mitogen-activated protein kinase
MARK3	microtubule affinity regulating kinase 3
MEK	Mitogen activated protein kinase
min	Minute
mL	milli Liter
mM	milli Molar
MOB	monopolar spindle-one-binder proteins
MOI	Multiplicity of infection
mRNA	Messenger RNA
MRTF	Myocardin related transcription factor
MST	Mammalian STE20-like (MST) protein
nd	Not determined
NF2	Neurofibromin

Abbreviation	Term
ns	Not significant
PAGE	polyacrylamide gel electrophoresis
PBS	Phosphate-buffered saline
PCR	Polymerase chain reaction
qPCR	Quantitative real-time PCR
RAF	Rapidly accelerated fibrosarcoma
RAS	Rat sarcoma virus
RNA	Ribonucleic acid
ROCK	Rho associated proteins
RPM	Rotations per minute
SARAH	Salvador Rassaf Hippo
SDS	Sodium dodecyl sulfate
shRNA	Short hairpin RNA
siRNA	Small interfering RNA
SMAD	Suppressor of mother against decapentaplegic
SRF	Serum response factor
SW1/SNF	Switch/sucrose non fermentable
T/E	Trypsin/ethylenediaminetetraacetic acid
TAO	Thousand and one amino acid kinases
TAZ	Taffazin
TEAD	Transcriptional enhanced associated domain
TEMED	Tetramethyl ethylenediamine
TFs	Transcription factors
TGF-β1	Transforming growth factor β1
Tris	Tris(hydroxymethyl)aminomethane
VEGF	Vascular Endothelial growth factor
VEGFR2	Vascular endothelial growth factor receptor 2
WT	Wildtype
YAP	Yes associated protein
ZO2	Zonnula occludent proteins
µg	Micro gram
µM	Micro Molar
µMACS	Magnetic associated cell sorting

Table 20 List of abbreviations

7.3   Index of figures

7.4 Index of tables

7.5 List of publications and conference contributions

7.5.1 Publications

- **Passi,M**, Vinay Kumar, and Gopinath Packirisamy. "Theranostic nanozyme: Silk fibroin based multifunctional nanocomposites to combat oxidative stress." Materials Science and Engineering: C 107 (2020): 110255.

- **Passi, M**., Shahid, S., Chockalingam, S., Sundar, I.K. And Packirisamy, G., 2020. Conventional And Nanotechnology Based Approaches to Combat Chronic Obstructive Pulmonary Disease: Implications for Chronic Airway Diseases. International Journal of Nanomedicine, 15, P.3803.

- **Passi,M**. And Zahler, S., 2021. Mechano-Signalling Aspects of Hepatocellular Carcinoma. Journal Of Cancer, 12(21), P.6411.

- CDK5 interacts with STK3 and modulates Hippo Pathway (PhD project, manuscript in preparation).

- Lorenz Isert, **Mehak Passi** et.al Cellular EMT-status governs contact guidance on electrospun TACS-mimicking in-vitro model (manuscript in preparation

7.5.2 Conference

- Poster presentation, Title '**CDK5 interacts with STK3 and modulates Hippo pathway'** -At Cell Bio 2022 (ASCB/EMBO joint event) in Washington DC, USA, 3rd- 7th December 2022.

7.6   Acknowledgements

First and foremost, I would like to express heartfelt thanks and gratitude to my Doktor Mutter and Doktor Vater, Prof. Vollmar and Prof. Zahler. I could not have achieved this without their constant supervision and support. I am very grateful to Prof. Zahler who not only gave me this wonderful opportunity to pursue my PhD studies at my dream University but also stood by my side and guided me throughout this journey and assisted me in every single step. He was always there for me whenever I needed his help ready to support and troubleshoot any problems, I had. He is my mentor. Prof. Vollmar on the other side with her warm nature always supported and encouraged me to go ahead and pursue the tasks courageously and proceed with my research work. Words fall short to express the respect and gratitude that I have for both of my PhD supervisors. They not only provided me with the resources for PhD but also accompanied me throughout this incredible journey and acted as a counsellor/therapist in times of need. They helped me become a better working professional and researcher ready to take on the world.

Next, I am heartily thankful to my Doctoral committee Prof. Koch, Prof. Wagner, Prof. Biel and Prof. Dr. Franz Paintner for being on my PhD examination committee. They all have been so kind., nice and humble.

Next, I am very much indebted to DAAD for providing me with the PhD scholarship to pursue Doctoral studies at LMU Munich. I would not have been able to do this without DAAD standing always by my side and supporting a young researcher like me and facilitating me to fulfil my dream and make a career.

Also, I would like to express my thanks to Jana and Bernadette especially. Bernadette always thawed my cells whenever I needed them and did maxi preps for me. Jana on the other hand helped me perform my experiments, especially at the end of my thesis writing. Apart from work, it was always nice talking to them and sharing with them other things about my life. Both have been angels to me, and I will always cherish the relationship that I have with them. I would also like to

especially thank Maibritt and Ling from my group. They always gave me really good ideas for my project and helped me if I had any problems with experiments. They became my very good friends in the lab. Apart from work I also understood a lot about German culture and laws from Maibritt which indeed helped me a lot through my PhD life in Germany and will continue to help me further. I also am very much grateful to Dr Jan Stöckl and Dr Thomas Froehlich from Gene Zentrum, LMU Munich who helped me perform phosphoproteomic analysis and acquire a large amount of paramount data for my project. I am also very thankful to Frau Schnegg for helping me with Western blots also.

Next, I am also very much grateful to lab members current and past, Andisheh, Adrian, Daniel, Chris, Patricia, Peng, Lucas, Christina, Rita, Elke, Flo, Franz, Julia, and Pauline. It was an amazing time that I spent with them in the lab and made good memories whether its during lab outings or at graduation parties. It was my pleasure working with them and sharing good times. I will always remember these times and my amazing life at the AK Vollmar group.

At last, I am very much indebted to my family (My mom, dad and brother), and friends back in India and in Munich (Dr.Vinay Kumar, Kapil, Manila, Gareema, Monika, Robert, Karin, Apoorva, Itisha Lavnaya and Aniket,) for believing in me and constantly, motivating me and never leaving me alone. It's because of their blessings and good wishes I can achieve this milestone.

In the end, I am very much thankful to God for giving me this honor. I will try to the best of my abilities to stand up to this honor of being granted a PhD degree and work in the field of health care. I will try to serve humanity and work for the betterment of society to the best of my abilities.